VOL. 5 No. 7 JULY 1940

Philips Technical Review

DEALING WITH TECHNICAL PROBLEMS
RELATING TO THE PRODUCTS, PROCESSES AND INVESTIGATIONS OF
N.V. PHILIPS' GLOEILAMPENFABRIEKEN

EDITED BY THE RESEARCH LABORATORY OF N.V. PHILIPS' GLOEILAMPENFABRIEKEN, EINDHOVEN, HOLLAND

OUTPUT AND DISTORTION OF OUTPUT AMPLIFIER VALVES UNDER DIFFERENT LOADS

by A. J. HEINS van der VEN.

621.396.645.331.018.7

Since the impedance of a loud speaker varies considerably with the frequency, it is not sufficient to know the power delivered by an output valve at a given distortion for the optimum loading resistance only. The influence of the magnitude and the phase angle of the loading impedance on the output, especially that of output pentodes, forms the subject of this article. The significance is discussed of the curves measured for the reproduction. The behaviour of the output pentode is compared with that of the output triode and tetrode. In conclusion the influence of inverse feed-back is demonstrated by means of two diagrams.

The power which can be delivered by an output amplifier valve, a pentode for instance with a given distortion, depends very much upon the impedance with which the valve is loaded. This can easily be understood by considering the idealized I_a-V_a diagram of a pentode, *fig. 1.* When the valve is loaded with a resistance R_a, the momentary values v_a and i_a of the anode voltage and current, respectively, lie on a line drawn through the operating point I_a, V_a with the slope $-1/R_a$ with respect to the V_a axis, as explained in an earlier article [1]): the load line. The amplitude described on this load line (for example, end points A and B on line a) depends upon the magnitude of the grid A.C. voltage, and the output is proportional to the area of the shaded triangle. As long as the grid A.C. voltage is sufficiently small, the vibration along the load gives a faithful representation of this. On line a, however, which corresponds to a low loading resistance, the amplitude of the anode alternating current permissible without distortion may not become larger than the value I_a of the anode direct current. In the same way, on line c for a high loading resistance the amplitude of the anode A.C. voltage may not become larger than the anode D.C. voltage V_a. If the grid voltage varies more than corresponds to these limits, which may be read off in the diagram, the tops of the curves for anode current and voltage would be cut off considerably, *i.e.* there would be strong distortion. The distortionless output is thus limited at low loading resistances by the anode current and, as appears from the corresponding triangle, it is given by $^1/_2\, I_a{}^2R_a$; with high loading resistance the output is limited by the anode voltage, and given by $^1/_2\, V_a{}^2/R_a$. From fig. 1 it may at once be seen that the largest possible value of the output is obtained when $R_a = V_a/I_a$: both anode A.C. voltage and current then have their maximum

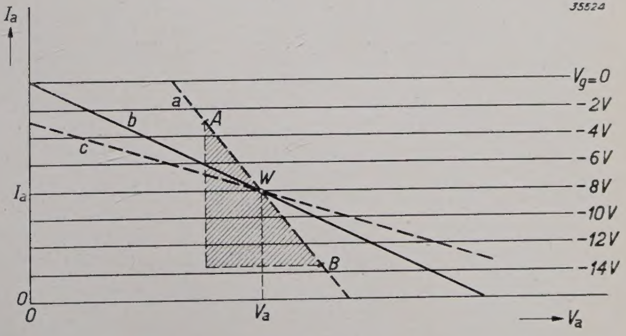

Fig. 1. I_a-V_a diagrams of an idealized pentode. The lines a and c are load lines for a low and a high loading resistance R_a, respectively. The amplitude AB along the load line is determined by the grid A.C. voltage, the shaded triangle gives the output. The reproduction is free of distortion as long as the amplitude of the anode A.C. (on line a) does not become greater than the anode D.C. I_a, or the anode D.C. voltage V_a, respectively. The output at different loading resistances is hereby limited. The limit lies highest for the "optimum" loading resistance $R_a = V_a/I_a$, line b.

---

[1]) A. J. Heins van der Ven, Testing amplifier output valves by means of the cathode ray tube. Philips techn. Rev. 5, 61, 1940. Figs. 3 and 12 have already been given in that article. We assume in every case here that the output valve operates in a class A amplifier connection, *i.e.* that the operating point is so chosen that the anode current never becomes zero at the normal grid voltage amplitudes.

values, and the output amounts to $^1/_2\ V_a\ I_a$. This loading resistance is called the optimum resistance, R_{opt}. For $R_a < R_{\text{opt}}$, according to the above, the maximum output is proportional to R_a, for $R_a > R_{\text{opt}}$, it is inversely proportional to R_a. In *fig. 2* this relation between output and loading resistance is represented graphically.

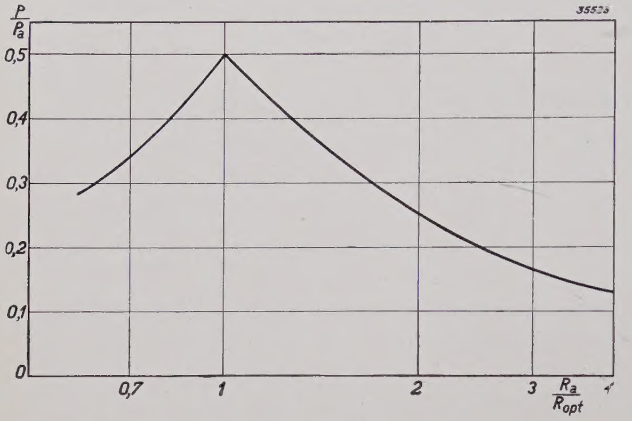

Fig. 2. For the ideal pentode the distortionless output is a maximum of $P = {}^1/_2\ I_a{}^2 R_a$ at loading resistances R_a smaller than the optimum R_{opt}, and the maximum $P = {}^1/_2\ V_a{}^2/R_a$ for $R_a > R_{\text{opt}}$. When $R_a = R_{\text{opt}} = V_a/I_a$ the limit is $P = {}^1/_2\ I_a V_a = {}^1/_2\ P_a$.

In order to characterize an output valve one often makes use of the power which the valve can deliver at a given distortion in the above-mentioned optimal loading resistance $R_{\text{opt}} = V_a/I_a$. In most practical cases, however, the output valve is not loaded with the optimal resistance, but with one or more loud speakers whose impedance varies as a rule very much with the frequency and moreover exhibits a certain phase angle. As an example the magnitude and phase angle of the impedance is given in *fig. 3* of a normal type of loud speaker as a function of the frequency. Considering this fact, it is important in judging an output valve to know the relation between output and distortion also at loads other than the optimum.

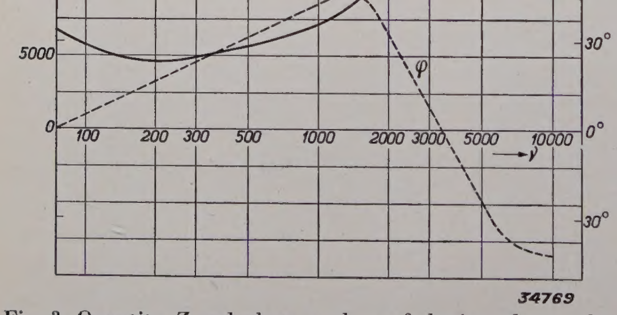

Fig. 3. Quantity Z and phase angle φ of the impedance of a normal loud speaker as a function of the frequency ν in c/s. As customary in receiving sets, in parallel with the primary winding of the loud speaker transformer there is a condenser of 2 000 μμF, which is responsible for the fall in the impedance at $\nu > 3\ 000$ c/s. At 1 000 c/s Z is about equal to the optimal loading impedance of the output pentode EL3 (7 000 ohms), while at 3 000 c/s Z has increased to about three times this value.

For the case of an ideal pentode we have already found the curves of fig. 2 for this purpose. These curves divide the surface of the whole diagram into two zones: at points below the limiting line there is no distortion, while the opposite is true at points above the line. In the case of an actual pentode there is no such sharp transition. The I_a-V_a diagram in this case differs from that of the ideal case in that the different characteristics (V_g = constant) are not at equal distances from each other, so that distortion already occurs before the above-mentioned limits can be reached. In *fig. 4* it may be seen that the sections which the successive characteristics intercept on the load line gradually become shorter, the farther away from the operating point one proceeds in both directions. This means that, with a purely sinusoidal grid A.C. voltage, harmonics occur in the anode A.C. voltage and current. This distortion might be investigated as a function of the amplitude along the load line (*i.e.* of the output), by measuring the sections intercepted on the load line. In practice, however, this method is too elaborate and too inaccurate. It is better to measure the quantities in question, output and distortion, directly. Several results of such measurements, chiefly on output pentodes, will be given and discussed in this article. First, however, we shall examine briefly the question of the quantitative measure which is used for the

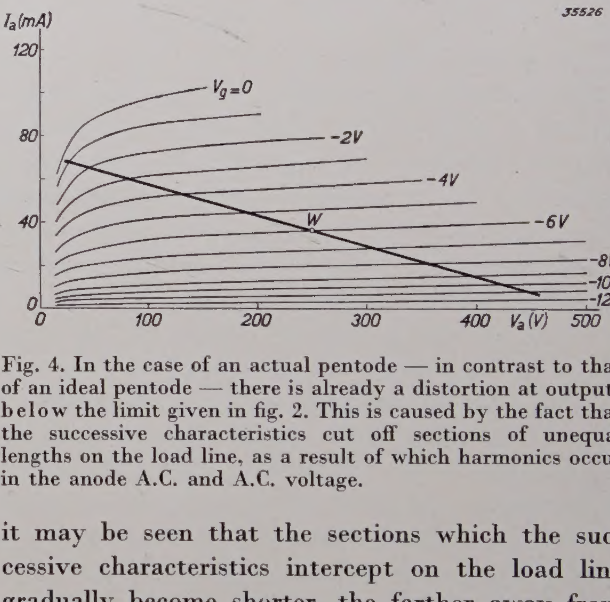

Fig. 4. In the case of an actual pentode — in contrast to that of an ideal pentode — there is already a distortion at outputs below the limit given in fig. 2. This is caused by the fact that the successive characteristics cut off sections of unequal lengths on the load line, as a result of which harmonics occur in the anode A.C. and A.C. voltage.

distortion and the magnitude of the latter which is permissible in practical cases.

Definition and permissible value of the distortion factor

As a measure of the distortion of an alternating current the "distortion factor" D is usually employed. This is defined as follows:

$$D = \sqrt{\frac{i_2^2 + i_3^2 + i_4^2 + \dots}{i_1^2}} \quad . \quad . \quad . \quad . \quad (1)$$

i_1 is here the purely sinusoidal current supplied as input signal, and i_2, i_3, i_4, ... the currents of the different harmonics occurring in the output signal. The denominator is sometimes written $i_1^2 + i_2^2 + i_3^2 + \dots$ instead of i_1^2. In practical cases where D is usually less than 10 per cent this makes no great difference.

If the factor D is used as a measure of the distortion, the quality of the reproduction must be better the smaller the value of D. This is in general in agreement with experience. There are, however, cases where the reproduction is very poor while only a small distortion can be measured. This is in particular the case when phenomena with a discontinuous character occur. When, for instance, a grid A.C. voltage which becomes positive for an instant at its peaks is supplied to the output valve of an amplifier, a grid current begins to flow at those instants. This sudden load on the preceding stage may, when it has not been taken into account, cause a distortion which is much more disturbing than would be concluded from the distortion factor measured.

In working with the factor D, therefore, one must first be sure that no discontinuous phenomena occur. In a complete receiving set it will sometimes be difficult to find this out without special means. In a simple low-frequency amplifier care must only be taken that no grid current flows in any of the valves and that the grid A.C. voltages do not assume such a value that the anode voltage remains zero during part of the period (see above).

How large may the factor D become? From the results obtained by different investigators [2]) it appears that it is usually sufficient for good reproduction if the distortion factor is smaller than 5 per cent. In a few very special cases the requirement may be made that the distortion factor should not amount to more than 1 to 1.5 per cent [3]), while for carrier-wave telephony for scientific investigations and calibrations (tone generators) the distortion may only amount to fractions of one per cent.

Influence of the magnitude of the loading resistance

In *fig.* 5 the relation between output distortion and load is represented graphically for the output pentode EL3. The curves show the output at a given distortion as a function of the loading resistance. (It is assumed for the present that the latter has the phase angle $\varphi = 0°$).

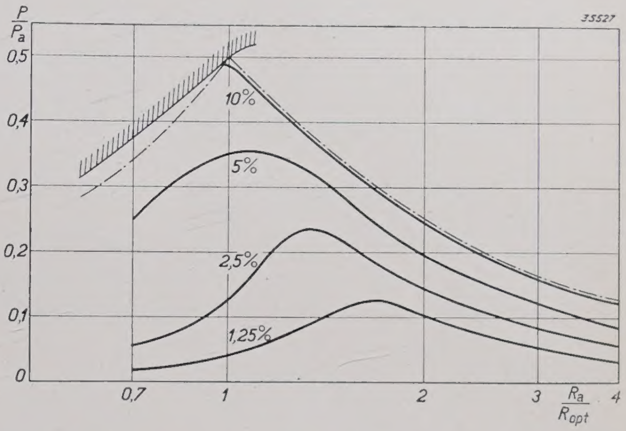

Fig. 5. The output P of the output pentode EL3 as a function of the loading resistance R_a with the distortion factor D as parameter. The unnamed quantities P/P_a and $R_a/R_{\rm opt}$ are plotted (the permissible value of $P_a = I_a \cdot V_a$ is 9 watts in this case; $R_{\rm opt}$ = optimal load, in this case 7 000 ohms). The broken lines indicate the limits for the distortionless output of an ideal pentode (fig. 2). In the case of the shaded line grid current begins to flow.

In order to make the diagram more easily comparable with similar diagrams of other valves, the output P and the loading resistance R_a are not themselves plotted, but P is referred to the power $P_a = I_a V_a$, which is converted into heat at the anode without grid A.C. voltage being supplied to the valve and R_a to the already mentioned optimum loading resistance $R_{\rm opt}$, as is indicated in fig. 2. Ordinates and abscissae are therefore the unnamed ratios P/P_a and $R_a/R_{\rm opt}$, respectively. The curve with the parameter value of $D = 5$ per cent represents the above-mentioned limit for "good quality", while in addition the curves for $D = 1.25$, 2.5 and 10 per cent are given.

The limiting curves of fig. 2 are also indicated by broken lines in the figure. These are valid for an idealized pentode. By means of these curves an idea is given of the degree to which the valve considered approaches the ideal case.

If such a high grid A.C. voltage is supplied to the valve that the limiting line drawn is exceeded, a region is entered in which the disturbing character of the distortion is no longer determined by D, since the anode current and voltage are cut off more or less discontinuously. Upon further increase of the amplitude of the grid A.C. voltage, the latter finally becomes positive at its peaks and grid current flows. The limit of this region is indicated in fig. 5 by the shaded line.

---

[2]) For instance: F. Massa, Proc. Inst. Rad. Eng. **21**, 682, 1933, and H. von Braunmühl and W. Weber, Akust. Z. **2**, 135, 1937.

[3]) H. G. Beljers, T. Ned. Radiogenootschap **6**, 115, 1934.

The reproduction of speech and music; comparison of pentode and triode

What conclusions may now be drawn from fig. 5 as to the reproduction with the output pentode considered? When the listener desires to increase the volume of the reproduction and does this by ear, he will proceed only so far that no disturbing distortion occurs in any frequency region in the case of music and speech. The average level which is reached in this way will depend upon the height of the peaks occurring in the music or speech and on their distribution over the frequencies. Suppose that the loud speaker has the impedance curve represented in fig. 3. A certain value of the loading resistance then corresponds to each frequency (we shall neglect the phase angle of the impedance in these considerations), thus at each loading resistance in the diagram of fig. 5 the average level must lie as far below the theoretical limiting line or below the line with the greatest permissible distortion as is required by the peaks occurring here. The value of R_a (the frequency) at which this restriction is most serious will depend upon the frequency spectrum of the sound reproduced and on the position of the line for the permissible distortion.

The average level may then in general be set higher, the higher the positions of the lines $D =$ constant, and in particular, the higher the limiting line where discontinuous phenomena begin to occur. With the optimum load this limit lies at about $P/P_a = 0.5$ for the valve EL 3, see fig. 5. When it is kept in mind that an average level of 0.2 watt already represents a very considerable volume of sound, and that the line $P/P_a = 0.022$ corresponds to this in the 9 watt pentode mentioned, it will be seen that there is still a very wide margin for the peaks.

For the sake of comparison a similar diagram is given in *fig. 6* for the output triode AD1 (combined with a valve EF6 as pre-amplifier valve). In this case the output at loading resistances greater than the optimum is sharply limited by the occurrence of grid currents (thus not so much by the distortion factor). The limit lies at about the same level as the curve $D = 5$ per cent for the output pentode considered (fig. 5); for the optimum load especially it lies at $P/P_a = 0.32$, thus considerably lower than the theoretical limit with the pentode. The difference in the way in which the output is limited offers an important practical advantage in the use of the pentode. Assume that the sound has been adjusted to the correct permissible volume by ear. In the case of the pentode, the ear has for instance used the curve $D = 5$ per cent as criterion and this was not exceeded at the greatest intensity observed during the adjustment. If afterwards the intensity becomes greater, the sound is indeed somewhat more strongly distorted, but there is still a gradual transition to the level at which discontinuous phenomena and the accompanying very disturbing distortion occur. In the case of the triode on the other hand, in making the adjustment, the ear has already been compelled to make use of the criterion that no grid currents began to flow at the greatest intensity observed. If in this case the intensity becomes greater still, for instance in *fortissimo* passages of the music, a sudden very unpleasant distortion may result.

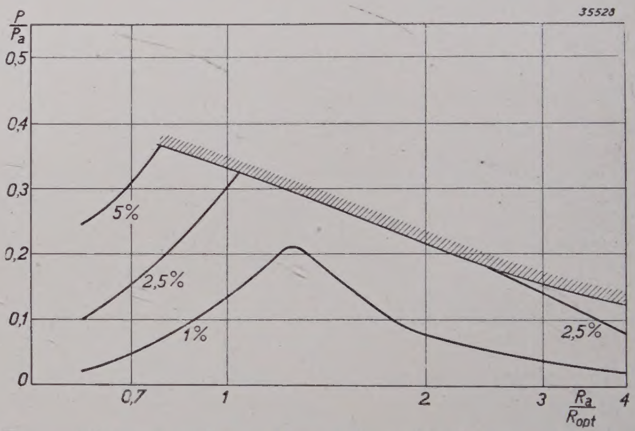

Fig. 6. Diagram similar to that of fig. 3 for the output triode AD 1 (combined with the pre-amplifier valve EF 6). The output is sharply limited by the occurrence of grid currents. The limit for $R_a = R_{opt}$ lies lower than with the output pentode.

Comparison of output pentode and tetrode

The fact, that in fig. 5 in the region $R > R_{opt}$ the curves run more or less parallel to the limiting line on which the amplitude v_a of the anode A.C. voltage has the maximum value V_a, indicated that when $D =$ constant here, v_a is also approximately constant, *i.e.* that the distortion is here mainly determined by the anode A.C. voltage and less by the magnitude of the loading impedance. In *fig. 7* where v_a is plotted as a function of R_a/R_{opt} for different values of D, this is expressed much more clearly. On the basis of the I_a-V_a diagram this behaviour is easily understood: if in fig. 4 the slope of the load line is slightly changed, from the optimum to larger values of R_a, the amplitude which can be described along the load line without touching zones of greatly deviating density of V_g curves, remains unaltered in the first approximation. A comparison of the pentode with a tetrode is interesting in this respect. As was briefly indicated in the article cited [1]), in tetrodes (in the modern types too, which more nearly resemble pentodes) the secondary emission from the anode to the screen grid cannot be entirely suppressed. This causes kinks in the I_a-V_a curves, see, for instance, *fig. 8.* If in such a diagram the load line for $R_a = R_{opt}$ is drawn it is seen that, upon a rotation of the line (increase of R_a), the sections of the line cut off by the V_g curves may rapidly become very unequal, see *fig. 9.* The distortion then increases very rapidly with R_a with equal amplitude along the line (amplitude v_a), or conversely for a given distortion the amplitude v_a of the anode A.C. voltage must become very much smaller. The broken line curves in fig. 7 show this clearly.

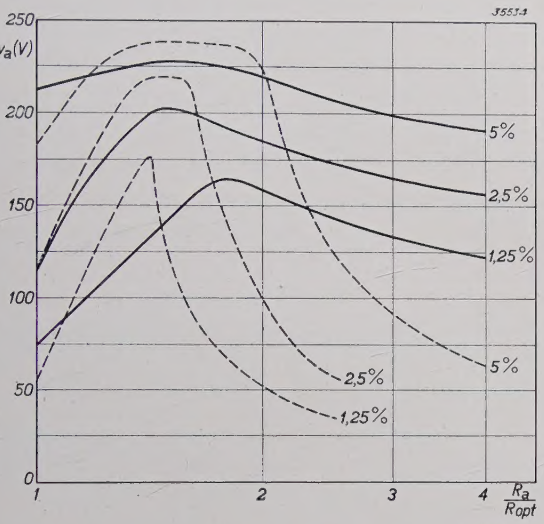

Fig. 7. In the region where $R_a > R_{opt}$ the distortion of an output pentode is mainly determined by the anode A.C. voltage v_a. The v_a curves here drawn for constant distortion therefore have a fairly long section practically parallel to the R_a axis. The broken line curves refer to an output tetrode which obviously behaves quite differently.

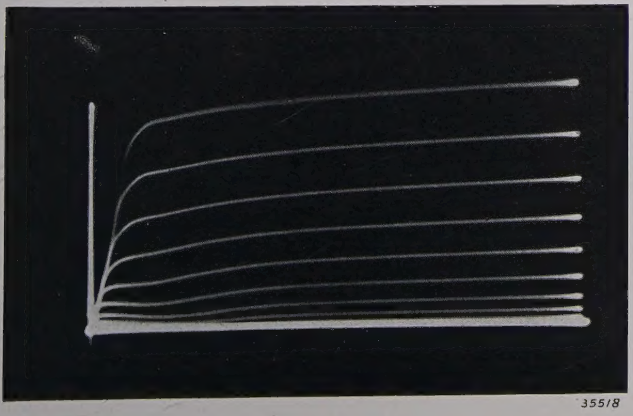

Fig. 8. I_a-V_a diagram of a tetrode.

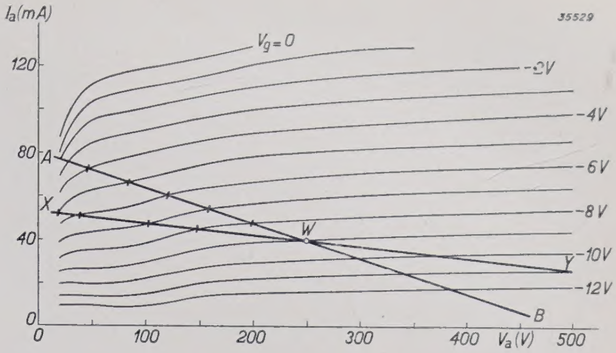

Fig. 9. Load lines for $R_a = R_{opt}$ (line AB) and for $R_a = 3 \cdot R_{opt}$ (line XY) in the I_a-V_a diagram of an output tetrode. The line AB is divided into almost equal sections by the successive curves for V_g = const. and therefore anode current and voltage vary practically linearly (at least according to an only slightly curved line) with the grid A.C. voltage. In the case of line XY, however, the sections cut off are very unequal in length: starting from the operating point W in the direction WX there is first a long section, then a much shorter one, then again a longer one and finally a short one again; the anode current and voltage here vary very irregularly with the grid A.C. voltage and a large distortion results.

Influence of the angle of the loading impedance

In the foregoing it has always been assumed that the loading impedance is a pure resistance, so that between the anode current and voltage there was no phase shift (straight load line). From the curve of fig. 3, however, it was found that in practice a phase shift must in fact be considered. If the phase shift φ is given different values successively, and in each case the output is measured as a function of the quantity Z with the distortion D as a parameter, a diagram like fig. 5 is again obtained, in which now, however, each curve for D = constant disintegrates into a set of curves for different values of φ.

Such a curve is given in *fig. 10.* The measurements are again carried out on the output pentode EL3,

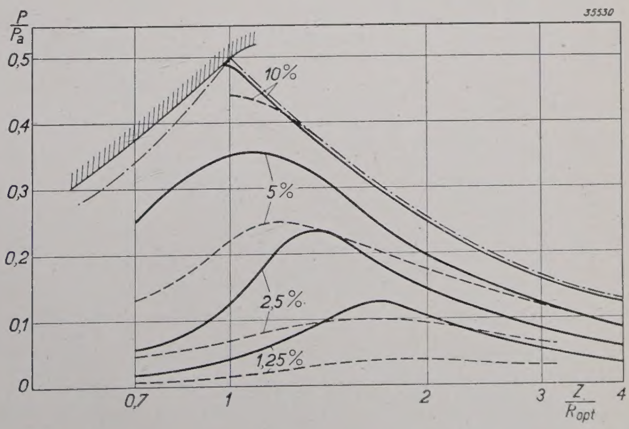

Fig. 10. Output of the output pentode EL3 as a function of the loading impedance Z. For each value of the distortion D a load with a phase angle $\varphi = 0°$ (full lines) and with a phase angle $\varphi = 45°$ (broken lines) is investigated. The phase shift between anode current and voltage is found to have an unfavourable effect on the output.

in which a self-induction and resistance in series was included in the circuit, while the distortion of the current in this circuit was measured. The phase shift amounted to $\varphi = 45°$ (dotted-line curves) and $\varphi = 0°$ (full-line curves), respectively. The latter curves are thus the same as in fig. 5. Not the true output $^1/_2\, i_a\, v_a \cos \varphi$, but the apparent output $^1/_2\, i_a\, v_a$ is plotted. For this reason the ideal limiting curve is the same for all values of φ, and in the curves obtained the influence of the valve properties only is expressed (not that of the work factor).

The figure shows that in the presence of a phase shift the output with a given distortion is considerably diminished. This may be explained as follows. The distortion may be chiefly ascribed to a second and third harmonic in the anode A.C., and we have already seen above that the occurrence of such is reflected in the inequality of the sections which the successive characteristics V_g = const. in the I_a-V_a diagram cut off on the load line. If the shortening of the sections takes place in the same way on both sides of the operating point, as is approximately the case with a straight load line with a slope close to the optimum, then the anode A.C. remains symmetrical, *i.e.* it contains no second harmonic. In *fig. 11* where the distortion due to the second and third harmonic, as well as the total distortion, is plotted as a function of the loading resistance, it may clearly be seen that due to this disappearance of the second harmonic in the neighbourhood of the optimal load the total distortion also reaches a minimum at this point. If the load is not a pure resistance, but the loading impedance has a certain phase angle, then the load line is not straight but elliptical (see *fig. 12*; without distortion it would be a true ellipse). Independent of the slope of the axis of this ellipse (magnitude of Z) the regions where the points of intersection with the characteristics begin to lie close together are always situated on parts of the ellipse which do not lie symmetrically with respect to the operating point. In this case therefore the second harmonic, and thus also the total distortion, always retain an appreciable value (fig. 11 broken-line curves). The curves which show the output at constant distortion will therefore be lower than in the case without phase shift.

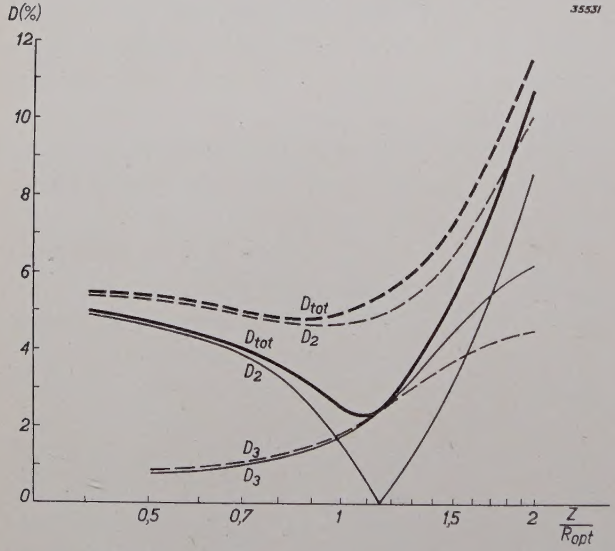

Fig. 11. The distortion factor of the output pentode EL3 is measured as a function of the magnitude of the loading impedance with constant grid A.C. voltage. The total distortion D_{tot} as well as the separate distortions D_2 and D_3, due to the second and third harmonics, respectively, are measured. The full line curves refer to the case where the loading impedance has the phase angle $\varphi = 0°$: in the neighbourhood of $Z = R_{\mathrm{opt}}$ the second harmonic disappears. The broken line curves are valid for $\varphi = 45°$; in this case D_2 is never equal to zero, D_{tot} is therefore always greater than for $\varphi = 0°$.

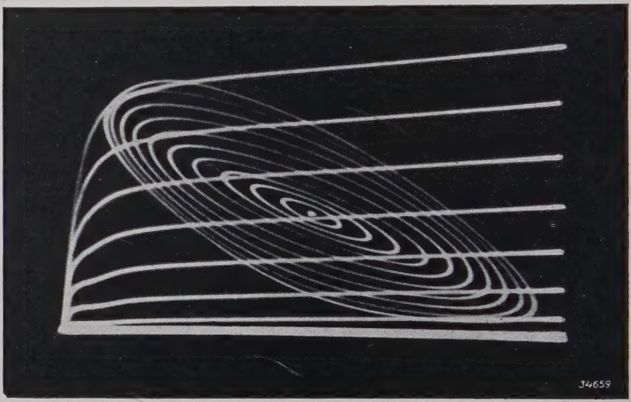

Fig. 12. With a phase shift between the anode current and voltage the load line in the I_a-V_a diagram (with sinusoidal grid A.C. voltage) becomes a more or less distorted ellipse about the operating point; the slope of the axis of the ellipse is given by the magnitude of Z, the loading impedance. In this case the amplitude of the grid voltage was varied by equal intervals.

Inverse feed-back

By the application of inverse feed-back, as repeatedly discussed in this periodical [4]), distortion of the reproduction can be decreased. This means that in figs. 5 and 10 the curves D = const. are all shifted to higher outputs. At the same time, however, it may be seen that the influence of the phase angle is eliminated to a considerable extent, so that the curves for $\varphi = 45°$ are much less unfavourable compared with those for $\varphi = 0°$. Even with the slight inverse feed-back which is obtained by omitting the condenser usually connected in parallel with the cathode resistance of the output valve, this may clearly be seen, as shown in *fig. 13*. About half of the amplification of the output stage is sacrificed in this inverse feed-back.

---

[4]) See for example, B. D. H. Tellegen, Philips techn. Rev. 2, 289, 1937.

A more usual form of inverse feed-back is that in which a voltage is conducted from the loud speaker or anode circuit of the output valve back to the grid of the pre-amplifier valve. This feed-back may be made proportional to the loud speaker current (current inverse feed-back) or to the loud speaker voltage (voltage inverse feed-back), by taking it off from a resistance either in series or in parallel with the loud speaker. *Fig. 14* gives the distortion diagram of the valve EL3 combined with the pre-amplifier valve EBC3 with the application of a "fourfold" voltage inverse feed-back. By this is meant that the amplification is reduced to $^1/_4$ of its value without inverse feed-back. It may be seen that with this relatively weak inverse feedback the output at a given distortion has become considerably greater, while at the same time a phase shift now no longer has any practical effect. The remaining difference in output at $\varphi = 0°$ and $\varphi = 45°$ with this voltage inverse feedback even has an opposite sign to that in the case of no feed-back.

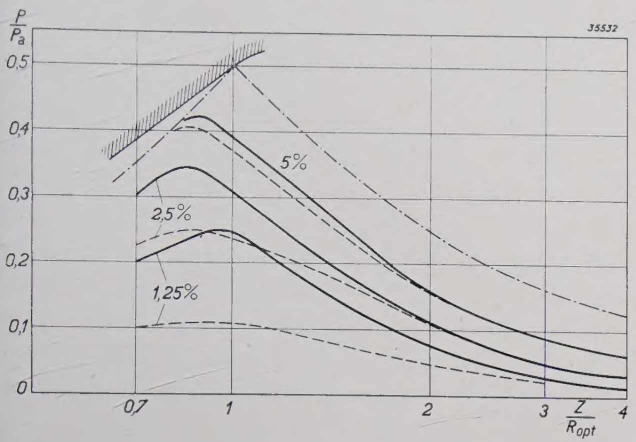

Fig. 13. Diagram similar to that of fig. 10 for the same output valve upon application of very slight inverse feed-back. The curves for a given distortion are higher than without inverse feed-back and the influence of the phase angle is less.

If, as in this case, no account need be taken of the influence of a phase shift, conclusions may be drawn directly from the above considerations about the adaptation to each other of loud speaker and output valve. The most important frequency region, *i.e.* that in which the most important contribution to the total sound intensity is delivered, lies in general in the neighbourhood of 1 000 c/s. Care should therefore be taken that the absolute value of the loud speaker impedance corresponds as nearly as possible in this frequency region to the optimal loading resistance of the output pentode. As may be seen, therefore, the loud speaker with the impedance curve given in fig. 3 is well adapted to the pentode EL3 whose optimum loading resistance is 7 000 ohms.

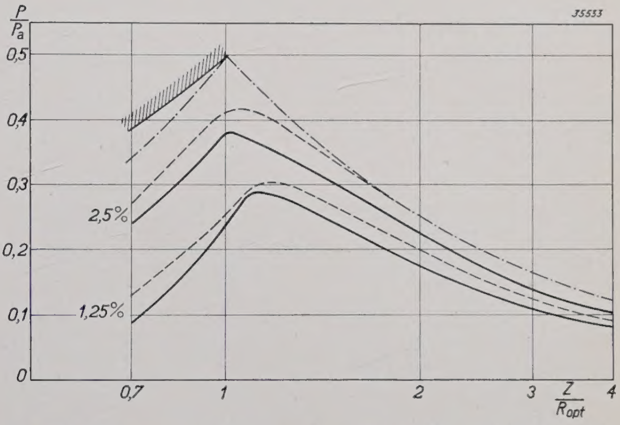

Fig. 14. Diagram similar to that of figs. 10 and 13 with the application of fourfold voltage inverse feed-back. The curves lie still higher than in fig. 13, and the difference for $\varphi = 0°$ and $\varphi = 45°$ has even changed its sign.

A PERMANENT MAGNET WHICH CAN LIFT 3 500 TIMES ITS OWN WEIGHT

by J. L. SNOEK.

621.318.22 : 669.15.018.58

The ratio between the lifting power and the weight of a magnet forms a better measure of the quality of the magnet steel than the lifting power alone. By the application of modern magnet steels a ratio of 3 500 has successfully been achieved. In this article the factors are discussed which must be considered in the construction of a magnet in order to make the ratio of lifting power to weight as large as possible.

In the early period of the development of permanent magnets and at the time when natural permanent magnets were scarcely exceeded in strength by artificial ones, a common test of the strength of a magnet was the measurement of its lifting power. One still finds in musea, besides natural magnets of reinforced magnetic iron ore, heavy magnets of carbon steel which are capable of lifting considerable loads. Considerations of technical advantage were scarcely taken into account in the making of such magnets; it was only a question of the demonstration of an interesting natural force which was rendered as large as possible by suitable means.

At the present time these demonstrations have lost much of their attraction, since it is commonly known that magnets of any desired lifting power could be made by increasing the dimensions of the magnet steel sufficiently. As to this increase, the technical possibilities are now practically unlimited, in any case an attempt to reach the limit of possibility would exceed the scope of a simple demonstration.

The question of the ratio between the maximum load which a permanent magnet can lift and the weight of the piece of magnet steel used is quite different. It will immediately be understood that this ratio provides a better criterion of the performance of the magnet steel than the size of the load lifted as such. Instead of making the load which a magnet can lift larger and larger, it is of more advantage to try to make the weight of the magnet which will lift a given load smaller and smaller. An example of such a demonstration which was given before the Natuur- en Geneeskundig Congres in Nijmegen in April 1939, is reproduced in *fig. 1*. An old magnet of 10 kg together with the maximum load it can lift (15 kg) was suspended from a modern permanent magnet with a suitable armature. The magnet steel of the latter magnet did not weigh more than 100 g.

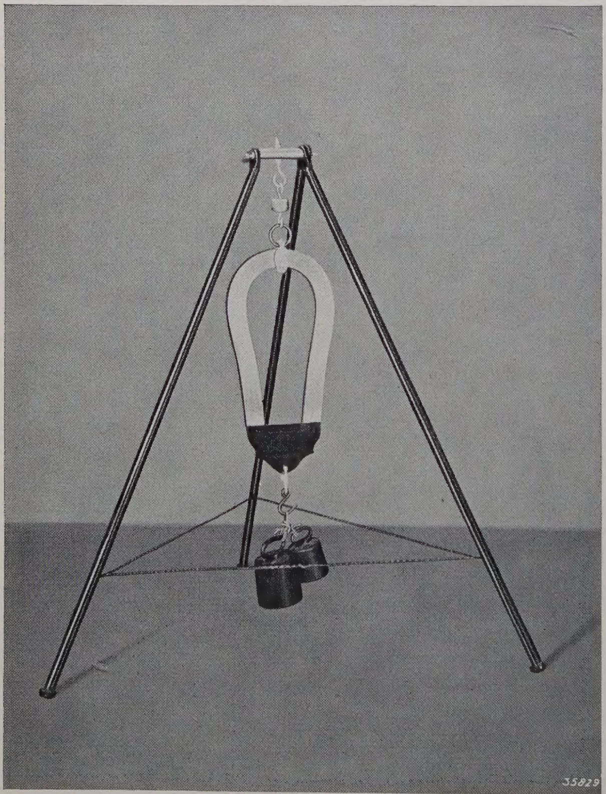

Fig. 1. Demonstration of the progress in the construction of magnets by improvement in the magnet steel. An old magnet of 10 kg (for which we owe thanks to Prof. Dr. A. D. Fokker of the Teylerstichting at Haarlem) with its maximum load (15 kg) hangs from a modern loud-speaker magnet, the steel of which weighs only 100 g.

Strictly speaking the ratio between lifting power and weight is also no pure measure of the qualities of a magnet steel, but is found itself to depend upon the absolute dimensions with a given shape and properties of the magnetic material. The force with which the armature of a magnet is held, with given inductions in the iron circuit, is proportional to the surface of contact between armature and magnet. Since the inductions which occur in the material are not changed upon proportional changes in the dimensions, we see that the lifting power is proportional to the square of the dimensions, while the weight increases with the cube of the dimensions.

The ratio would therefore be more favourable the smaller the dimensions are kept. There is, however, a technical limit to the reduction of the dimensions, due to the accuracy with which the connected parts of the magnetic circuit can be worked. If for instance the ground surfaces are not absolutely plane and smooth, there is an air gap between the parts which has a certain magnetic resistance. If moreover a kind of iron with a permeability of $\mu = 4\,000$ is used for the pole pieces, the resistance of an air gap of 1 micron corresponds to that of 4 mm of soft iron, and it is therefore very difficult to make the dimensions of the iron circuit smaller than, for example, 1 cm without the induction being so much lowered due to the transition resistance in the air gap, that the ratio between lifting power and weight also begins to become smaller.

At definite dimensions of the magnet, therefore, the ratio between lifting power and weight will reach a value which cannot practically be exceeded, and which in turn is determined in the first instance by the quality of the magnet steel.

By the application of modern types of magnet steel it has been found possible to construct a magnet which can lift 3 500 times its own weight (see *fig. 2*). The kind of steel used is "Ticonal" 3.8 with a remanence of 12 000 gauss and a coercive force of 550 oersted. The pole pieces consist of an alloy of 50 per cent cobalt and 50 per cent iron. This alloy has a higher magnetic saturation than pure iron, and at a field strength of only 5 oersted it reaches an induction of 19 000 gauss. The surface of contact between the armature and the pole pieces amounts to only 0.1 sq.cm; the lifting power is 1.65 kg. Since the magnet steel used — a cube of edge 4 mm — weighs only 0.47 g, a ratio of 3 500 is achieved.

It will perhaps be of interest to learn how this tiny magnet was designed.

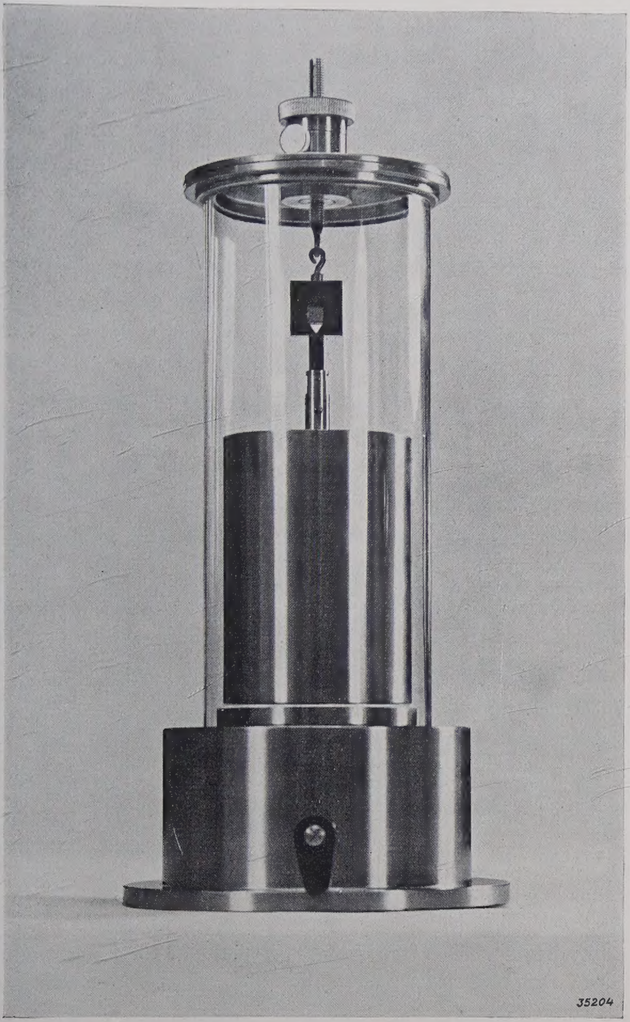

Fig. 2. A magnet which can lift 1.65 kg and the steel of which weighs only 0.47 g.

Construction of the magnet

The lifting power of a magnet is given by

$$K = \frac{1}{8\pi} \int B_n^2 \, \mathrm{d}f,$$

where B_n is the component of the magnetic induction which is perpendicular to the surface of contact between magnet and armature, and df is an element of this surface. If S is the area of the surface, then in the case of a homogeneous induction

$$K = \frac{1}{8\pi} B_n^2 \cdot S = \frac{1}{8\pi} \frac{\Phi^2}{S} ,$$

where Φ is the flux of the magnet. From this formula it follows that with a given magnetic flux it is advantageous to constrict the bundle of lines of force as much as possible at the position of the surface of contact.

In order to make the surface S small it is desirable to use for the pole pieces and the armature a material which has a very high magnetic saturation. As stated, an alloy of cobalt and iron was employed whose magnetic saturation is 15 per cent higher than that of pure iron. By carefully annealing the material, magnetization nearly to saturation can be achieved in a field of several oersted.

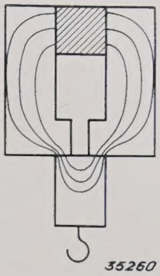

Fig. 3. Principle of the construction of a magnet with great lifting power. The magnet steel is shaded.

In *fig. 3* the principle of the construction is shown. The magnetically hard material is shaded while the soft material is left white. The surface of contact between the pole pieces and the armature is made as small as possible; it must, however, remain large enough to cause practically the whole flux to pass through the armature and not through the air gap between the pole pieces. This air gap may not be made arbitrarily wide, but must be so narrow that the magnet retains its full strength upon pulling off the armature [1]).

When the dimensions of the air gap and the surface of contact of the armature are determined, the optimum dimensions of the magnet steel can also be determined. The cross section must be sufficiently large to magnetize the armature to the optimum value, while the length must be so great that the remanence of the magnet upon pulling away the armature does not fall too suddenly. These two requirements, however, as well as the above mentioned factors concerning the proportions of air gap and surface of contact, cannot be expressed directly in formulae so that it is impossible to calculate the optimum dimensions. It is better to determine them experimentally.

Fig. 4 shows how this is done. Two rectangular pieces of cobalt-iron 4 mm thick were separated by a copper foil 0.1 mm thick. These pieces were clamped in a frame of V2A steel, and the whole soldered together with solder having a high melting point to give a strong unit.

---

[1]) If L is the length of the magnetically hard material and l the width of the air gap, then upon pulling away the armature there occurs in the steel a demagnetizing field $H_i = Bl/L$. (See A. Th. van Urk, Philips techn. Rev. **5**, 29, 1940). l must be made so small that this field causes practically no decrease in the remanence.

A groove was then cut as shown in fig. 4*b*. The most favourable apex angle of the V-shaped groove was studied experimentally and amounts to about 60°.

The upper part of the groove, in which the magnet steel will be inserted later, was temporarily closed with a suitable piece of V2A steel in order to be able to heat it without deformation.

The magnet steel is now introduced (fig. 4*c*), and when in position magnetized by holding it in the field of an electromagnet. The V2A steel is then ground away from the lower side, and determinations of the force of attraction for armatures of different shapes are begun. With a sufficiently great length of air gap (copper foil) this is at first only slight. By grinding off thicker and thicker layers from the under side (if necessary with heat treatment between successive grinding processes in order to remove tensions) the length of air gap at which the attractive force is a maximum can be determined experimentally. Fig. 4*d* gives the form finally reached.

As may be seen from the figure, the piece of magnet steel bears absolutely no load. The cube which is ground beautifully smooth, is so loose in the groove that it can le pushed away with a pencil. Nevertheless it is of course responsible for the flux which causes the force between the pole pieces and the armature.

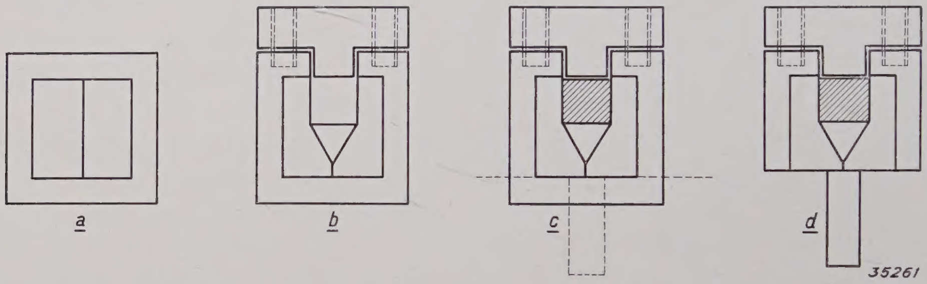

Fig. 4. Construction of the magnet shown in fig. 2.

a) Two pieces of cobalt-iron, separated by a copper foil, are soldered into a frame of V2A steel.

b) A groove is cut in the piece, which will later contain the magnet steel. The groove is temporarily closed with a small piece of V2A steel and the whole is heated to free it of tensions.

c) The piece of magnet steel is inserted. The whole is magnetized in the field of an electromagnet, and with different armatures the force of attraction is determined which is obtained after grinding away the lower part of the frame of V2A steel.

d) More and more material is ground away on the lower side until the lifting power has reached a maximum.

The ratio obtained of 3 500 between lifting power and weight would have been considered unattainable several years ago. The experiments which were carried out in the development of the magnet described, however, confirm the impression that the result obtained by no means represents an upper limit, and that twice this ratio could be reached if the experiments were continued [2]). Although the construction and the material of the pole pieces contribute very much to the attainment of this favourable result, it may nevertheless be said that the progress which has become possible in recent years is mainly to be ascribed to the improvement in magnet steel. A simple estimation shows that with equal care in construction with a carbon steel less than one tenth of the ratio would be reached which is obtained with the modern steel.

---

[2]) In the meantime a ratio of 5 000 was obtained with another construction. The absolute lifting-power, too, in this case was considerably increased *viz.* 65 kg with a weight of magnet-steel of only 13 g.

THE USE OF SELENIUM VALVES IN RECTIFIERS

by D. M. DUINKER.

621.314.634

Due to the danger of breakdown or overheating, the voltage and current, respectively, on a blocking-layer valve are limited. In this article these limits are derived by means of the dynamic characteristics of the valves, with special reference to the selenium valves manufactured by Philips. The allowable peak voltage in the blocking period amounts to 35 volts. From this follows the permissible transformer voltage in various rectifier connections. The allowable direct current can be read off from a graph for different form factors; it amounts to 4.4 to 6.6 amp. for selenium valves of 90 cm² effective surface with cooling plates. The connection of valves in series and in parallel is discussed. From the properties of the valves (counter EMF and resistance) the external characteristic of the rectifier can be derived. This is explained by means of examples and one practical example is treated numerically.

The construction and operation of blocking-layer valves, in particular the selenium valves manufactured by Philips, has already been dealt with in this periodical [1]). Since these valves, compared with mercury-cathode valves and hot-cathode valves, have the advantage that they need no attention at all when in operation and are always ready for use, they are particularly suitable in rectifiers for the supply of telephone mains and other signaling arrangements. In addition to this, in rectifiers for all other purposes such as the charging of accumulator batteries, galvanic chromium plating, etc. blocking-layer valves are being more and more commonly used.

In designing a rectifier one begins with the requirement that it shall be able to give a certain current and voltage. The number of valves, necessary for taking care of this, is determined by the maximum voltage and current values permissible for one valve. In the following we shall consider the selenium valve in this respect, and, more generally, its application in different rectifier connections.

In order to make clear the restrictions set to the voltage and current of a blocking-layer valve, we must recall the construction of such valves. They are built up of a semi-conductor and a metal, between which there is a thin insulating or blocking layer (*fig. 1*). Such a combination has the property that an electric current experiences a greater resistance in the direction from the metal to the semi-conductor ("blocking direction") than in the opposite direction ("transmitting direction"). In the case of selenium valves a layer of selenium deposited on a metal base plate is used as semi-conductor. By a heat treatment the blocking layer is formed on the free surface of the selenium; upon this, as metal, an alloy is finally spread which must have a lower melting point than selenium. One or more connecting wires are soldered to the metal layer, while a second contact is connected to the base plate.

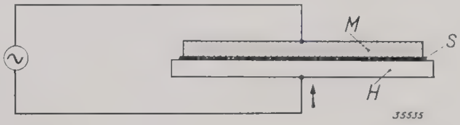

Fig. 1. Diagram of a blocking-layer valve. *M* metal, *S* insulator (blocking layer, with a thickness of the order of magnitude of 10^{-5} cm), *H* semi-conductor. The arrow indicates the transmitting direction.

The limits of the load on the valve are now determined by the fact that with too high a voltage a breakdown of the blocking layer occurs, while with too high a current too great heating, and thus fusion of the alloy used occurs. Although neither of these two phenomena need make the valve immediately useless, it will nevertheless be clear that they should be avoided as far as possible.

The current-voltage characteristic

The limits mentioned for the current and voltage will be derived in the following with the help of the current-voltage characteristic of the valve, the principle of which is illustrated in *fig. 2*. In the ideal case the resistance in the transmitting direction is zero and in the blocking direction infinite, *i.e.* the ideal characteristic coincides with the upper vertical and left-hand horizontal coordinate axes. Actually a small current also flows in the blocking direction; this "leakage current", however, increases at first very slowly, but from a certain voltage on, very rapidly with increasing voltage, which indicates that with a slight further increase of the voltage breakdown will occur. This voltage may be taken as the permissible limiting value. In the transmitting direction also the characteristic deviates from the ideal, due to the fact that the resistance does not become exactly zero. The energy consequently lost as heat in the valve causes the abovementioned rise in temperature which increases with the current. If the relation between the losses in the valve and the rise in temperature is known (determined by the cooling), the permissible losses can be determined, and from that, by a method to be discussed later, the permissible current can be determined with the help of the current-voltage characteristic.

---

[1]) W. Ch. van Geel, Blocking layer rectifiers, Philips techn. Rev. 4, 100, 1939. In this article we shall use the term "rectifier" for a complete arrangement and shall indicate the rectifying element of the circuit by the term "valve".

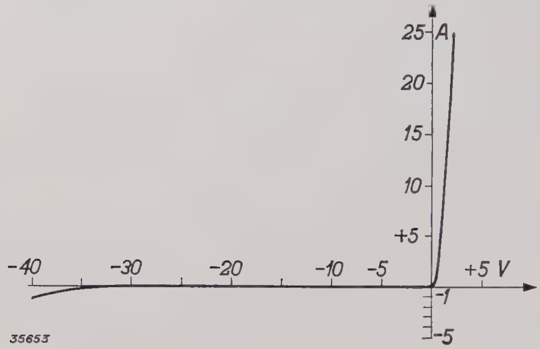

Fig. 2. Current-voltage characteristic of a selenium valve. In the ideal case the characteristic coincides with the left-hand and upper vertical coordinates.

We have continually spoken of "the" characteristic, and one might thus be inclined to think of a relation obtained by the successive application of different voltages and measurement of the current in each case. The current values given by such a "static" characteristic may, however, differ appreciably from those occurring during operation. Upon application of a voltage in the blocking direction the current reaches a final value ²) only slowly, which value — aside from its being reproducible only with difficulty — will certainly not correspond to the momentary value occurring upon the application of a rapidly alternating voltage. The characteristic for the transmitting direction will also be different with static measurement than during operation of the valve, when transmitting and blocking states alternate with each other. It is therefore necessary to record the characteristics of valves under conditions as far as possible like normal operating conditions. The most suitable method for this is with the cathode-ray oscillograph, by means of which the desired "dynamic" characteristic (relation between the momentary values ³) of current and voltage) can be made directly visible. The connections used for this are given in *fig. 3*. It must here be noted that it is not possible to record the characteristic for blocking and transmitting directions simultaneously. If the deviations from the ideal case, with which we are here concerned, are to be made visible on a reasonable scale, a small scale for the voltage and a large one for the current are needed for the blocking direction, where the voltages are high and the currents low, and for the transmission direction, just the opposite. It is therefore desirable for practical reasons to record the two parts of the characteristic separately. The way in which this is done is explained in the text under fig. 3.

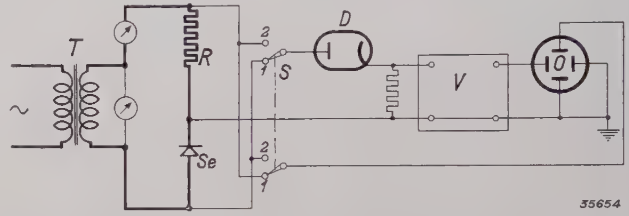

Fig. 3. Connections for recording the dynamic characteristic of selenium valves. The valve *Se* is fed from the transformer *T* and loaded with the (induction-free) resistance *R*. Blocking and transmitting characteristics cannot be recorded at the same time, since quite different scales are required. For the transmitting characteristic the switch *S* is set at *1*. The voltage on *R* is hereby conducted to the plates for vertical deflection of the cathode ray oscillograph *O*, so that the vertical deflection is proportional to the valve current. The valve voltage, after the diode *D* has suppressed the high voltage peaks in the blocking direction, is amplified with the amplifier *V* and applied to the plates for horizontal deflection. For the blocking characteristic *S* is set in position *2*. The (high) blocking voltage on *Se* now acts directly on the plates for vertical deflection, the voltage decay along *R* is conducted to *V via* the diode *D*. The diode now transmits only the low voltage on the resistance *R*, which is caused by the leakage current; the horizontal deflection is thus proportional to the leakage current. By connecting several valves (six, for instance) in series, a five to tenfold amplification in *V* is sufficient for obtaining a reasonable size of image. The average characteristic of the six valves is then measured.

Permissible voltage

In *fig. 4* two characteristics recorded for a Philips selenium valve for the blocking direction are shown,

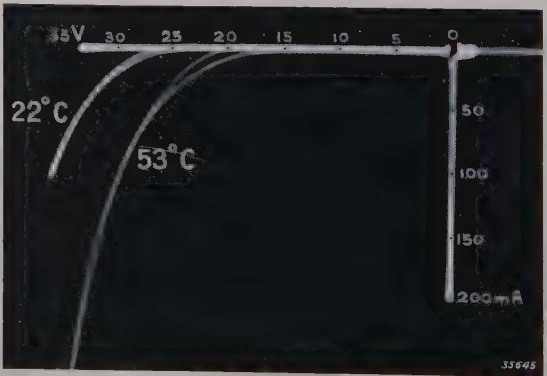

Fig. 4. Blocking characteristic of a selenium valve with an effective surface of 90 cm², at different temperatures.

---

²) See the article cited in footnote ¹).

³) It is clear that this relation must depend to a certain extent upon the frequency of the A.C. voltage used for the measurement, because at sufficiently low frequencies it must gradually take over the form of the static characteristic. The characteristics used in this article refer to frequencies of about 50 c/s.

as obtained at different temperatures of the valve. At the higher temperature the "leakage resistance" is found to decrease. The voltage, however, at which the leakage current begins to increase very rapidly, and above which therefore there is danger of breakdown of the blocking layer, is found to be about the same for all temperatures; it amounts to about 35 to 40 volts. The peak value of the alternating voltage on the valve may therefore be raised to about 35 volts, which may be considered a very high value for blocking-layer valves.

Table I

	A	B	C	D	E	F
1	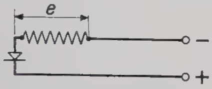	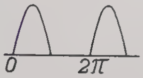	$2\sqrt{2}$	$n=$ 1	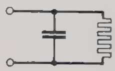	$f=$ 2 à 2,5
2	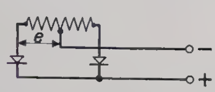	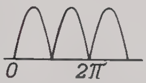	$2\sqrt{2}$	2	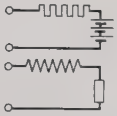	ca. 2 ca. $\sqrt{2}$
3	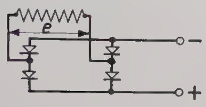	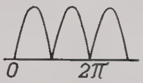	$\sqrt{2}$	2	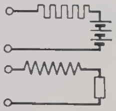	ca. 2 ca. $\sqrt{2}$
4	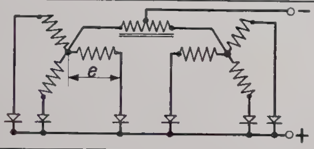	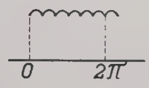	$2\sqrt{2}$	6		$\sqrt{3}$
5	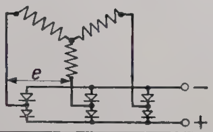	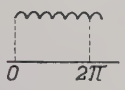	$\sqrt{2}$	3		$\sqrt{3}$

35669

In column *A* several customary rectifier connections are given: *1* is the simplest, single-phase connection, *2* the two-phase star connection, *3* the three-phase Grätz connection (by which the A.C. voltage is rectified in both halves of the period), *4* a six-phase rectifier with a so-called interphase transformer, *5* the three-phase Grätz connection. Column *B* shows the form of the rectified voltage. Column *C* gives the ratio between the peak voltage which acts on one valve at no-load and the effective transformer voltage (e). Columns *D*-*F* are only spoken of later on in this article. *D* gives the number of contributions to the current which come together at each connection terminal, which can easily be counted in the sketches of column *A*, column *E* gives several commonly occurring types of loading, *F* the rough values of the form factor f of the valves hereby occurring. With a larger number of phases, as in the connections *4* and *5*, the form factor does not depend so closely on the load.

From the permissible peak value, the voltage which may be applied to the valves in different rectifier connections can now be deduced. In *Table I* the relation is given for a number of ordinary rectifier connections (column *A*), between the peak voltage on each valve and the effective transformer voltage e (column *C*; for the meaning of e see the diagrams). From this it follows that for the connections *1*, *2* and *4* the permissible voltage $e = 12.5$ volts, and for connections *3* and *5* $e = 25$ volts. Since the permissible peak value of 35 volts must not be exceeded, it is advisable to make the limit for the nominal transformer voltage lower by a factor equal to the ratio of the highest mains current occurring to the nominal mains current.

If the desired D.C. voltage demands the application of higher A.C. voltages e, recourse must be had to the connection in series of a number, s, for instance, of valves. If these valves all had exactly the same blocking characteristic, the same blocking voltage would act on all the valves, since the same leakage current flows through them all. Actually, however, there is always a certain divergence in the properties of the valves, so that the total blocking voltage will be divided more or less unevenly among the valves connected in series. In order to be able to keep this irregularity within narrow limits, the valves are sorted into groups after manufacture: in each group the leakage current, measured with a given voltage applied, exhibits a given maximum deviation from a mean value, characteristic of the group. By connecting in series valves of the same group only, in the most unfavourable case one of the s valves will only have to carry a voltage about 18 per cent higher than the total voltage divided by s. This voltage must remain below the permissible value of 12.5 and 25 volts, respectively. The permissible transformer voltage e which may safely be applied to the s valves connected in series is thus $0.85 \cdot s \cdot 12.5$ volts (or $0.85 \cdot s \cdot 25$ volts).

One peculiarity must be noted when a selenium valve is used alternately at different voltages. The blocking characteristic is not unchangeable, but varies according to the magnitude of the mean blocking voltage. The lower the latter the smaller the leakage resistance [4]). The variation takes place very slowly upon lowering the voltage (the change is only noticeable after several days); upon increasing the voltage, on the other hand, it takes place relatively quickly (in a few minutes). The result is that a valve which has operated for days at a low voltage (for instance at less than $^1/_4$ of the maximum permissible voltage), and is then suddenly connected to a much higher voltage, exhibits temporarily an abnormally high leakage current. After a few minutes, however, the characteristic has become adapted, and the leakage current has sunk to the ordinary value.

Permissible current

In order to find the limit of the direct current which a valve can give, we must, as already mentioned, examine the losses in the valve. The losses are made up of two parts: the loss w_d caused by the resistance experienced by the current in the transmitting direction (effective current); and the loss w_s caused by the flow of leakage current in the blocking state. The blocking loss w_s is found to amount to only 5 to 10 per cent of the transmitting loss w_d in normal use. We shall therefore first examine only the latter.

Losses in the transmitting direction

The power ω_d dissipated in the valve can be calculated at each moment as the product of current i and voltage v_d. The average wattage loss $\overline{w_d}$ is found by integrating w_d over one period T of the supply A.C. voltage and dividing the result by T:

$$\overline{w_d} = \frac{1}{T}\int_0^T i \cdot v_d \, \mathrm{dt} \quad . \; . \; . \; . \quad (1)$$

v_d is given as a function of i by the dynamic characteristic for the transmitting direction, which is shown in *fig.* 5 recorded for three different temperatures. For a given temperature and not too low currents, the characteristic can be sufficiently accurately represented by:

$$v_d = v_0 + i \cdot r, \quad . \; . \; . \; . \; . \quad (2)$$

where the quantities v_0 and r, which are independent of the current, may be considered as "counter EMF" and resistance of the valve, respectively. *Fig.* 6 shows how v_0 and r are determined from the characteristic recorded with the oscillograph; in the example given $v_0 = 0.9$ volt, $r = 0.07$ ohm (this value holds for a selenium valve of about 90 cm² effective surface; v_0 is independent of this surface, r inversely proportional to it).

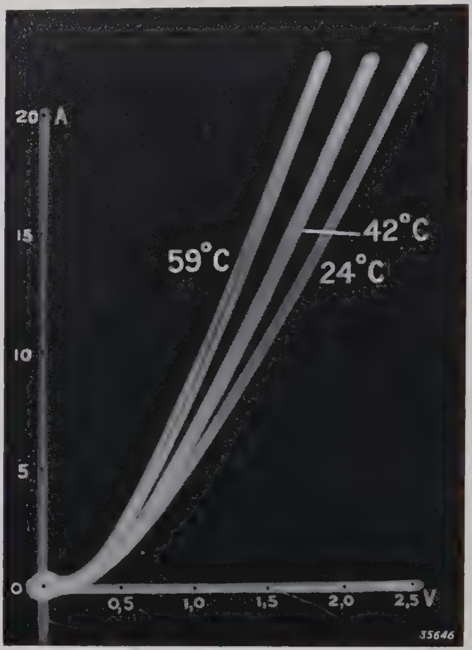

Fig. 5. Transmitting characteristic of a selenium valve (90 cm² effective surface) at different temperatures.

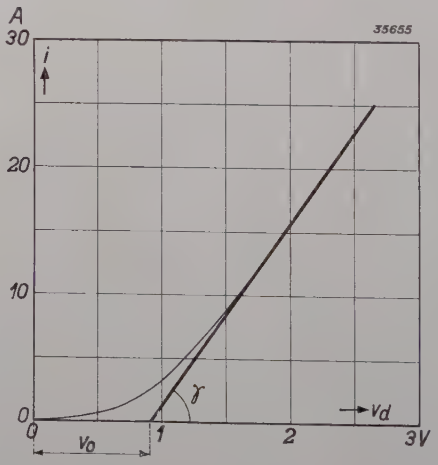

Fig. 6. The transmitting characteristic for not too small current amplitudes is approximately a straight line: the valve has, as it were, a counter EMF v_0 and a resistance r (= cot γ).

---

[4]) Such a phenomenon also occurs in the case of electrolytic condensers. See W. Ch. van Geel and A. Claassen, Philips techn. Rev. **2**, 65, 1937.

From (1) and (2) it follows that:

$$\overline{w_d} = v_0 \cdot \frac{1}{T}\int_0^T i\,\mathrm{d}t + r \cdot \frac{1}{T}\int_0^T i^2\,\mathrm{d}t = v_0\bar{i} + r i^2_{\mathrm{eff}} \quad (3)$$

Here $\bar{i}$ is the average value, i_{eff} the effective value of the current rectified by the valve. Equation (3) may also be written in a somewhat simpler form by introducing the ratio between i_{eff} and $\bar{i}$, the so-called "form factor", f, which may to some degree be considered as characteristic of the form of the current [5]):

$$\overline{w_d} = v_0\bar{i} + r f^2\, \bar{i}^{\,2} \quad . \ . \ . \ . \quad (4)$$

In *fig. 7* this ratio between wattage loss and direct current is represented graphically for different form factors f. For v_0 and r the values of the example in fig. 6 are here taken.

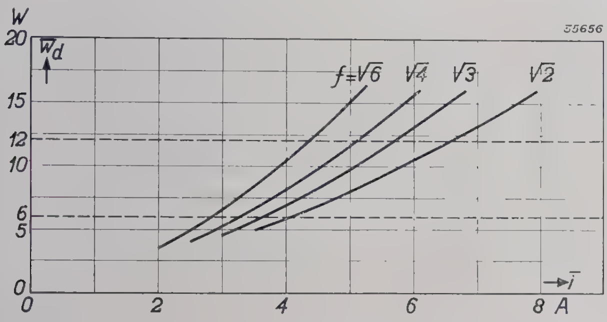

Fig. 7. Wattage loss $\overline{w_d}$ in the transmitting direction as a function of the mean direct current $\bar{i}$, calculated according to formula (4) for different values of the form factor f as parameter.

Permissible dissipation in the valve

What now is the value of the direct current $\bar{i}$ with which the valve may be loaded? In order to discover this we must know the relation between the losses in the valve and the rise in temperature which they cause. This relation, which naturally depends upon the method of cooling the valve, has been determined experimentally and is given in *fig. 8* for valves *a*) without special provision for cooling, and *b*) with cooling plates (see *fig. 9*). The permissible temperature of the valves has been determined to be 65 °C with a reasonable margin of safety. With an arrangement such that the air flowing along the valves has not been pre-heated by any other source of heat, a maximum initial temperature of 35 °C in non-tropical countries may be assumed, so that the rise in temperature due to the losses may amount to 30° C. According to fig. 8 this corresponds to a loss of 13 watts without cooling plates. From these limits for the permissible loss $\overline{w_d}_{\mathrm{max}}$, the permissible direct current $\bar{i}$ through the valve may be found with different forms of current (form factors f) by finding the point of intersection of the curves drawn in fig. 7 with the line $\overline{w_d} = \overline{w_d}_{\mathrm{max}}$ (this line actually lies somewhat lower than 7 and 13 watts, respectively, as we shall see in the following).

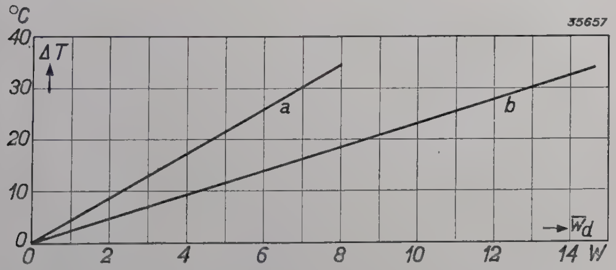

Fig. 8. Rise in temperature ΔT of a selenium valve (90 cm² effective surface) mounted in the ordinary way, as a function of the energy dissipated; *a*) without cooling plates, *b*) with cooling plates (aluminium, 20 × 20 cm, 2 cm thick).

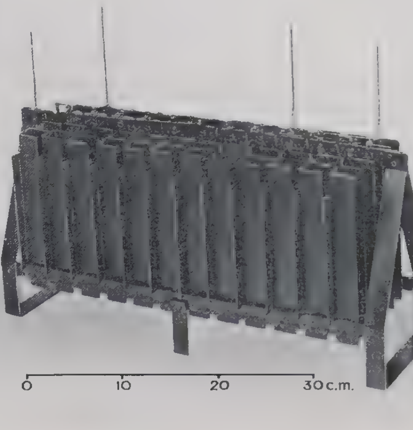

Fig. 9*a*. Valves (with cooling plates) of a Grätz rectifier according to table I, *3*. Where each valve stands in the diagram there is a group of three selenium valves (90 cm² surface) in series; thus $s = 3$, $p = 1$. With this rectifier 21 cells of a lead accumulator in series can be charged with a maximum charging current of 10 amp.

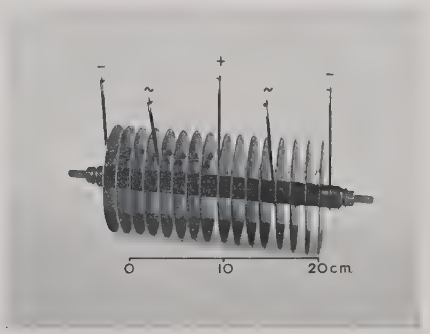

Fig. 9*b*. Valves (without cooling plates) of a similar Grätz rectifier; here, however, $s = 4$, $p = 1$. 28 lead cells in series can be charged with a maximum current of 6.5 amp.

---

[5]) The form factor is always larger than unity and usually lies between 1.4 and 2.5; for flattened curves it is lower than for pointed ones.

The values of v_0 and r by which the shape of the curves in fig. 7 is determined, still depend very much upon the temperature, as was indeed to be concluded from the appreciable difference between the three characteristics of fig. 5. Because of this dependence on temperature — in *fig. 10* the limits are given between which may lie the values of v_0 and r, which are quite different for different valves — the curves of fig. 7 are actually valid only for one temperature, which would have to be provided for the valve artificially by making different cooling conditions for every value of i. The method described of determining the permissible value of $\bar{i}$, gives the correct result when the curves are drawn specially for the temperature 65 °C. This temperature is just reached with a dissipation $\overline{w}_{d_{\max}}$ with the cooling conditions present when the valve is in use.

The values of v_0 and r chosen for fig. 7 are somewhat larger than ever occur at 65 °C (see fig. 10). At smaller values of v_0 and r according to (4), w_d will only reach the value $w_{d_{\max}}$ at a larger value of i. The permissible direct current values at $w_{d_{\max}}$ read off from fig. 7 are therefore on the safe side.

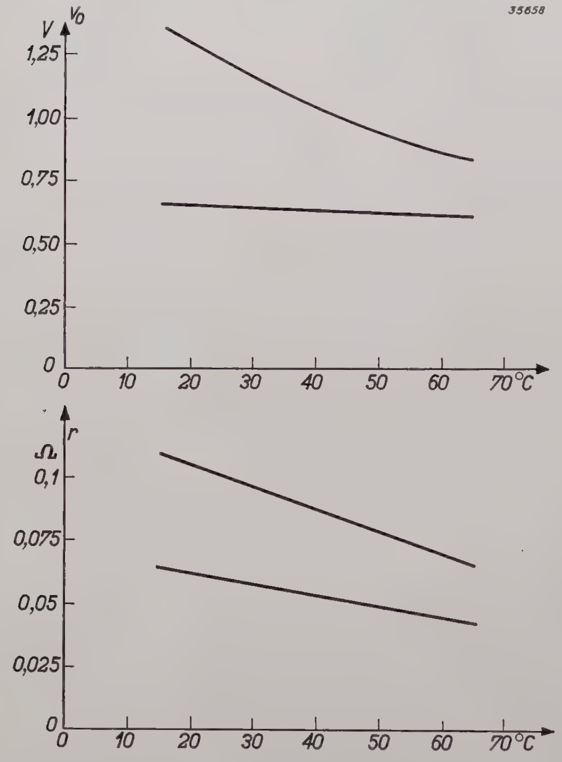

Fig. 10. Counter EMF v_0 and resistance r of selenium valves as a function of the temperature. The values of r are for 90 cm² effective surface (v_0 is independent of the surface). The two curves indicate approximately the extreme values occurring.

Losses in the blocking direction

A correction must now be introduced into these considerations because of the energy loss w_s due to the leakage current. An equation similar to (1) holds in this case:

$$\overline{w_s} = \frac{1}{T}\int_0^T i_l \cdot v_s \, \mathrm{d}t, \quad . \quad . \quad . \quad . \quad (5)$$

where i_l is the leakage current and v_s the blocking voltage. The variation of i_l as a function of v_s is given by the blocking characteristic (fig. 4). It is not as easy to express this in a formula as was the case with the transmitting characteristic. It is therefore simpler to plot the momentary values $w_s = i_l \, v_s$ as a function of the time and to integrate graphically or planimetrically.

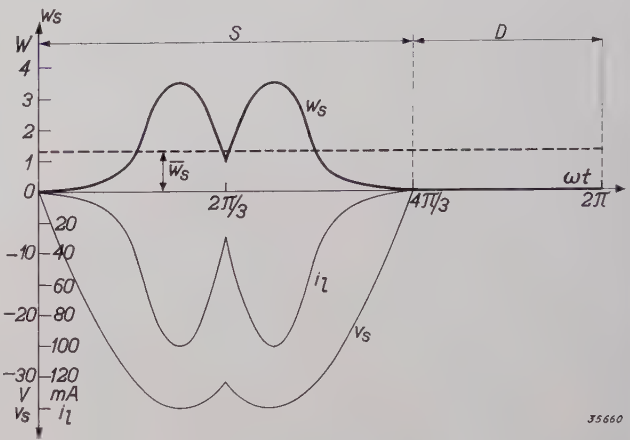

Fig. 11. Variation of the blocking voltage v_s on a valve in the three-phase Grätz connection (5 in table I). With the help of the blocking characteristic (fig. 4) the variation of the leakage current i_l may be calculated from this, and by multiplication of v_s with i_l the variation of the energy dissipated w_s can be constructed; $\overline{w_s}$ is the mean value of this wattage loss, S blocking interval, D transmitting interval.

If we first consider the no-load state, the blocking voltage v_s is given at every moment by the no-load voltage of the transformer. The variation of v_s is thus known for every connection. In *fig. 11*, for example, the variation of v_s is given for the connection 5 in table I (so-called three-phase Grätz connection). With the help of the leakage current with time, i_l can be constructed from this. The variation of i_l can of course also be recorded directly, with the help of an oscillograph (*fig. 12*). By multiplying the momentary values of v_s and i_l by each other, the variation of the blocking loss

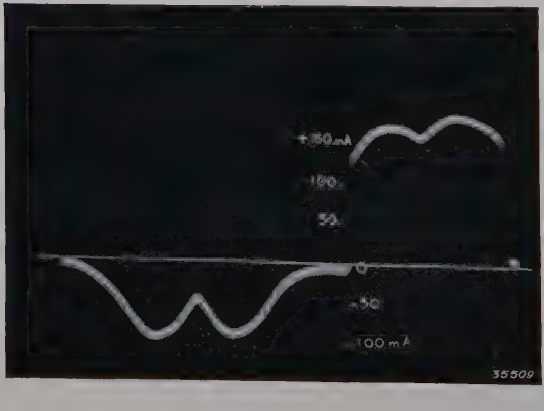

Fig. 12. Oscillogram of the leakage current for the case dealt with in fig. 11. The current agrees satisfactorily with that indicated in fig. 11.

w_s may be found (see fig. 11), the average value of which, w_s, may be determined by integration. In the example of fig. 11 at $e = 25$ volts (the maximum permissible voltage) $\overline{w_s} = 1.3$ watts. In the case where $e = 21$ volts one finds only $\overline{w_s} = 0.6$ watt. The great difference may easily be understood from the rapidly accelerated growth of the leakage current at the highest permissible voltages (fig. 4).

When the rectifier is loaded the blocking loss is less than with no load, due to the voltage loss caused in the valves when they are just in the transmitting period, and sometimes in impedances connected in front of the valves (we shall return to this later) by the loading current in the transformer. We are therefore perfectly safe if we calculate a value of, for instance, 1 watt for the blocking losses $\overline{w_s}$ during operation. By subtracting this energy from the permissible dissipation found from fig. 8, we finally obtain for the permissible loss in the transmitting direction, at a maximum air temperature of 35 °C, $\overline{w_d} = 12$ watts (with cooling plates) and 6 watts (without cooling plates).

The direct current obtainable

With these values of $\overline{w_d}_{\max}$ we now find in fig. 7 as permissible direct current $\overline{i}_{\max}$ for a valve of 90 cm² surface, according to the form factor f ($\sqrt{6} > f > \sqrt{2}$), a value between 4.4 and 6.6 amp. (with cooling plates) and between 2.8 and 4.1 amp. (without cooling plates). The total average current $\overline{I}$ which a rectifier in one of the connections of table I can give is found by multiplying $\overline{i}_{\max}$ by the number of contributions to the current n which come together at the positive or negative terminal of the external connection. This number, which can easily be counted in the sketches of column A, is given in column D of table I. In column F are given several approximate values of the form factor f in the connection in question and with the type of load sketched in column E.

If a direct current $\overline{I} > n\,\overline{i}_{\max}$ is required, then in the place of every valve in the connection used p valves must be connected in parallel. Just as when the valves are connected in series, the irregularity in the distribution of the current among the p valves must here also be taken into account. Here also the irregularity is limited by sorting the valves after manufacture into groups in which the voltage loss v_d measured at a given current i deviates by a few per cent at the most from a mean value. When valves of the same group only are connected in parallel, in the most unfavourable case one of the p valves has to take up a current about 18 per cent higher than the total current divided by p. By making this equal to the permissible maximum it is found that the current obtainable with p valves amounts to $0.85 \cdot p \cdot \overline{i}_{\max}$.

It must still be noted that the permissible direct current derived from fig. 7 is for selenium valves in continuous operation. With intermittent loading higher values are permissible, since the limitation is only a question of temperature. The heat capacity of the valve is then also of influence.

The above-mentioned phenomenon of a temporarily diminished "leakage resistance" upon switching a selenium valve to a high voltage after a long period of operation at a low voltage is also accompanied by a temporary increase in the blocking loss. In such a case therefore it is advisable, in order to prevent overheating, to wait a few minutes before changing over to full current load.

The external characteristic of rectifiers

We have shown in the foregoing, how, from the maximum permissible blocking voltage, the transformer voltage is derived to which a given arrangement of valves can be connected. How high must the transformer voltage be chosen to obtain the required D.C. voltage? To find this the voltage loss in the whole circuit, particularly that in the valves themselves, must be taken into account. This voltage loss, and with it the D.C. voltage obtained, varies with the rectified current (equation (2)). For many applications it will be important to know the relation between the D.C. voltage delivered and the direct current produced. This relation, the so-called external characteristic, may be affected by the connection in series of suitable impedances, and adapted to the purpose for which the rectifier is used.

We shall explain some of these points by means of a few examples.

Three-phase Grätz connection

In the rectifier connection *fig. 13a* (No. 5 of table I) the three coupled voltages of a three-phase main are rectified in both the positive and negative half of a period, so that a D.C. voltage with a six-phase ripple occurs at the output terminals (fig. 13*b*). Each of the six sine tops has a maximum at $e_0 = e\sqrt{2}$ and a width $\pi/3$, so that the average D.C. voltage becomes:

$$\overline{U}_0 = 6 \cdot \frac{1}{2\pi} \int_{\pi/3}^{2\pi/3} e_0 \sin \omega t \, \mathrm{d}(\omega t) = \frac{3}{\pi} e_0 \quad . \qquad (6)$$

This expression holds for the case where the possible counter EMF of the load is never greater than U_0 at any moment. If it were greater, the valve just about to come into action would be in the blocking state instead of in the transmitting state, and we would not be able to integrate over the whole sine peak. If we exclude this case, *i.e.* if the counter EMF is always smaller than $e_0 \sin \pi/3$, it would follow from (6) that the D.C. voltage is independent of the current $\bar{I}$. No account is here taken of the internal voltage loss in the valves, however. (The voltage loss in the transformer may here be neglected).

In the position of every valve in fig. 13*a* there may be a group of p branches in parallel each having s valves in series. Since equation (2) is valid for each valve, it is easy to see that the relation between the momentary value of the voltage v and the current i through such a group is given by:

$$v = s\left(v_0 + i\frac{r}{p}\right), \quad . \quad . \quad . \quad . \quad . \quad (7)$$

where v_0 and r are the average counter EMF and resistance of one valve. In the connections of fig. 13*a* the direct current always flows through two valve groups in series and there causes a voltage loss $\Delta U = 2\,s\,(v_0 + \bar{I}\,r/p)$. The average D.C. voltage is thus actually:

$$\bar{U} = \frac{1}{2\pi}\int_0^{2\pi} (e \sin \omega t - \Delta U)\,\mathrm{d}(\omega t) =$$

$$= \bar{U}_0 - 2s\left(v_0 + \frac{r}{p}\bar{I}\right) = \left(\frac{3}{\pi}e_0 + 2\,sv_0\right) - 2\frac{s}{p}r\bar{I} \quad (8)$$

In fig. 13*c* this relation is represented. The rectifier behaves, as far as direct current and D.C. voltage delivered are concerned, like a source of voltage with the EMF $3e_0/\pi - 2\,sv_0$, and the internal resistance $2\,sr/p$ (when we neglect the resistance of transformer and connections).

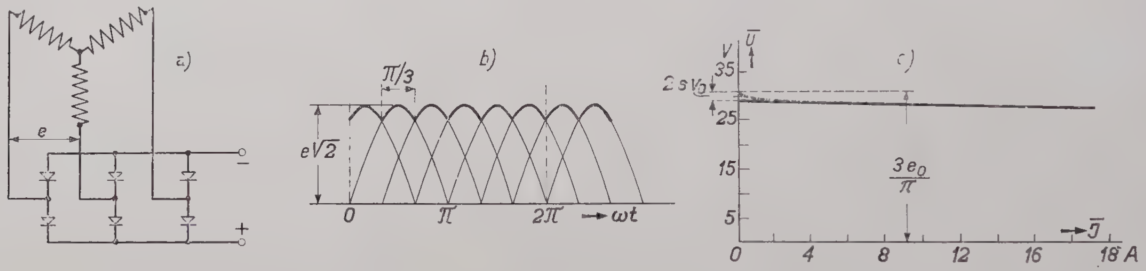

Fig. 13. *a*) Rectifier in three-phase Grätz connection (5 in table I).
b) The D.C. voltage delivered consists of the tops of six sine curves with maxima $e_0 = e\sqrt{2}$, and $\pi/3$ in width. The lowest value of the voltage occurring is $e_0 \sin \pi/3$.
c) External characteristic: mean D.C. voltage $\bar{U}$ as a function of the mean direct current $\bar{I}$ given. For the valves it is assumed that $v_0 = 0.6$ volt and $r = 0.05$ ohm. Transformer voltage $e = 22.5$ volts.

Fig. 13*c* is drawn to scale for the case where $p = 1$, $s = 1$, $v_0 = 0.6$ volt, $r = 0.05$ ohm, $e = 25$ volts. As could be seen from fig. 6, however, the approximation formula (2) and (7) used for the dynamic transmitting characteristic of the valves can only be applied with sufficiently high current, for instance $i > 7$ amp. in the figure (more generally with a current density greater than about 80 mA/cm²). With smaller currents the voltage loss in the valve is smaller than that given by the formulae; and consequently the external characteristic in fig. 13*c* will also deviate from a straight line according to (8) at small loads, and will vary according to the broken-line curve.

Single-phase Grätz connection

For charging accumulator batteries the simpler Grätz connection *fig. 14a* is often used (No. *3* in table I), with which a single-phase alternating current is rectified in both halves of the period. The rectified voltage (fig. 14*b*) here consists of two half sine curves $e_0 \sin \omega t$. In this case, due to the fact that the voltage periodically falls back to zero, we have just the case which was excluded in the first example, namely that due to the counter EMF U_t in the circuit, the charging current can only flow as long as $e_0 \sin \omega t > U_t$. If R_t is the total resistance of the circuit the momentary value of the current is given by:

$$I = \frac{e_0 \sin\omega t - U_t}{R_t} \quad . \quad . \quad . \quad . \quad . \quad (9)$$

The average value of the charging current is found by integration:

$$\bar{I} = 2 \cdot \frac{1}{2\pi}\int_{\alpha}^{\pi-\alpha} I\,\mathrm{d}\,(\omega t),$$

where α indicates the moment when I becomes zero, thus $\sin \alpha = U_t/e_0$.

The essential difference from the first example is therefore that the limits of integration depend upon the method of loading (the counter EMF U_t). Integration gives:

$$\bar{I} = \frac{2e_0}{\pi R_t}\left(\sqrt{1-\left(\frac{U_t}{e_0}\right)^2} - \frac{U_t}{e_0}\cos^{-1}\frac{U_t}{e_0}\right) \quad . \quad (10)$$

The relation thus found between $\bar{I}$ and U_t, the charging characteristic of the rectifier, is graphically represented in fig. 14*c*; in order to make the curve generally valid the unnamed numbers $\bar{I}\,\pi\,R_t/2e_0$ and U_t/e_0 are plotted.

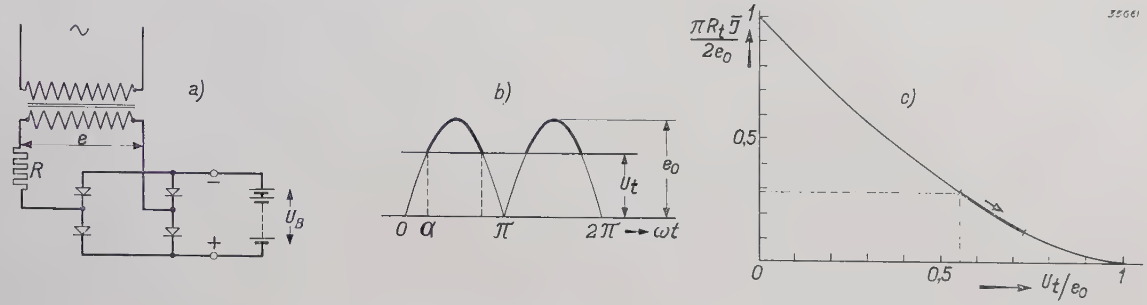

Fig. 14. *a*) Charging rectifier in single-phase Grätz connection (*3* in table I). The series resistance R, by which the charging current is reduced to the desired value, can be situated either on the alternating current side (as here indicated) or on the direct current side. The former connection has the advantage that in operation the full transformer voltage $e_0 \sin \omega t$ does not act as blocking voltage on the valves, but only that voltage diminished by the voltage loss in R. This also makes the leakage current smaller.

b) Variation of the rectified voltage. Charging current is delivered only at moments when $e_0 \sin \omega t$ is larger than the counter EMF U_t in the circuit (this is mainly the voltage of the battery to be charged).

c) Charging characteristic (relation between average charging current I and counter EMF U_t (battery voltage). The quantities $I\,\pi\,R_s/2e_0$ and U_t/e_0 are plotted. If it is required that with an increase in the counter EMF in the ratio 2.7 : 2.0 a decrease in the charging current to one half shall take place, the part of the characteristic indicated by a heavy line must be used, with an abscissa of 0.56 and an ordinate of 0.28 at the beginning. The required value of e_0 and R_t can be calculated from this.

What value must now be chosen for the transformer voltage (e_0) and the circuit resistance (R_t) in order to have the charging proceed as desired? The counter EMF U_t consists chiefly of the battery voltage U_B, which increases gradually during charging (with lead accumulators from about 2.0 to 2.7 volts per cell), so that according to fig. 14*c* the charging current falls. Now it is desirable on the one hand to begin with a high charging current in order to keep short the total time necessary for charging, while on the other hand it is desirable that toward the end of the process of charging, the current is automatically — *i.e.* without it being necessary to change e_0 and R_t — so decreased that the accumulator plates are not injured by excess gas development. In practice it is found that both requirements can be met when the initial and final currents are in the ratio 2 : 1. It follows from the charging characteristic that for this to be true, with a ratio 2.7 : 2.0 between the counter EMF at the end and that at the beginning, the abscissa at the beginning must be

$$U_t/e_0 = 0.56 \quad . \; . \; . \; . \; . \; . \quad (11)$$

and the ordinate:

$$\pi R_t\, I/2e_0 = 0.28 \quad . \; . \; . \; . \; . \quad (12)$$

Now we have seen in the first example discussed (equation (8)) that the valves give a counter EMF $2\,sv_0$ (the charging current passes through two valve groups in series each time) which is added to the battery voltage U_B; therefore

$$U_t = U_B + 2\,sv_0 \quad . \; . \; . \; . \; . \quad (13)$$

Furthermore the internal resistance of the two groups of valves is $2\,sr/p$, therefore

$$R_t = R + 2\,sr/p \quad , \; . \; . \; . \; . \; . \quad (14)$$

when R is the remaining circuit resistance, *i.e.* the series resistance plus the resistance of the transformer, the connections, etc.

With the help of equations (11) to (14) and the required charging current, e_0 and R_t can now be calculated. Assume that a battery of 24 lead cells in series must be charged with a rectifier for which $p = 1$ and $s = 4$; for the selenium valves, v_0 may be 0.6 volt and $r = 0.05$ ohm. The charging current I must be 10 amp. at the beginning and 5 amp. at the end. Equation (13) gives $U_t = 24.2 + 8 \cdot 0.6 = 52.8$ volts. From this with equation (11): $e = e_0/\sqrt{2} = 52.8/0.56 \cdot \sqrt{2} \approx$ *67 volts*. Furthermore equation (12) gives: $R_t = 0.28 \cdot 2 \cdot 67 \cdot \sqrt{2}/\pi \cdot 10 = 1.69$ ohms. Finally with the help of equation (14) one finds: $R = 1.69 - 8 \cdot 0.05 \approx$ *1.3 ohms*. If the internal resistance of the transformer, etc. is subtracted from this, the resistance is obtained which must be connected in series.

If we apply to this numerical example the consideration about the permissible voltage on the valve, we see that the rectifier was generously proportioned in this respect. The blocking voltage e acts on $s = 4$ selenium valves in series; according to the above discussion e may here reach the value $0.85 \times 4 \times 25 = 85$ volts. With the value of 67 volts to be chosen there is a generous margin of safety for mains voltage fluctuations. As to the current in this example where $p = 1$ and $f \approx 2$ (see table I), the current per valve group with cooling plates may amount to about 5.1 amp., (fig. 7), the total direct current $\overline{I}$, therefore, to 10.2 amp. (because $n = 2$, see table I). The desired initial charging current of 10 amp. is therefore just permissible.

From these examples it will be clear how the properties of the selenium valves are taken into account in designing a rectifier.

MEASUREMENT OF PHASE ANGLES WITH THE HELP OF THE CATHODE RAY TUBE

by W. NIJENHUIS. 621.317.3:621.385.832

Various methods are used for the measurement of phase angles between two voltages. Several of these methods are discussed briefly. A new method is then described which permits rapid and easy measurement, which covers the whole region from 0 to 360° and with which an accuracy of 2° can be attained. In this method the phase difference is measured by the difference in position of a luminous semi-circle on the screen of a cathode ray tube. The manner is described in which the circular motion of the fluorescent spot and the sharp limitation of the semi-circle, required for reading off the results, is obtained. The apparatus constructed in the Philips laboratory can be used for voltages of 6 mV to 3 V and for frequencies from 100 to 100 000 c/s. In conclusion a few sources of possible error in measurement are discussed.

In many alternating current problems phase angles, either between current and voltage in an impedance or between input and output voltages in the case of quadripoles, etc., play an important part. In high current technology the significance of the phase angle in the form of the work factor is well known. As to low current technology, we may refer to telephony, where phase shifts caused by transmission lines may affect the intelligibility (phase distortion ¹)); to television where the video-frequency signals must be transmitted strictly true to phase; and finally to radio and amplifier technology where phase problems are continually to be dealt with. An instructive and less generally familiar example of such a problem is discussed in the present number of this periodical ²), namely the influence of the phase angle of a loud-speaker impedance on distortion and output of an output amplifier valve.

How are such phase angles measured? As long as it is a question of determining the phase angle of a complex impedance, bridge connections can be used with which the real and imaginary parts of the impedance can be measured separately. For the more general case where the phase of a given alternating current or A.C. voltage is required with respect to another current or voltage there are numerous methods. We shall here describe a method worked out in this laboratory which makes use of a cathode ray tube. For a better understanding, however, it is first desirable to give a brief survey of several other methods used until now, in which a cathode ray tube was also used.

Various methods of measurement

A very simple determination of phase shifts is made possible by the use of an electron switch ³). By this means the variation with time of two voltages (or currents) can be made visible simultaneously on the screen of a cathode ray oscillograph (*fig. 1*), so that the relative phase shift — difference in time between corresponding points — can be measured directly. The accuracy is in this case naturally limited. The error may amount for instance to from 5 to 10°.

Other methods work with Lissajous figures: the two voltages are applied to the two sets of deflection plates of a cathode ray tube. If the frequencies of

---

¹) See for instance Philips techn. Rev. 4, 20, 1939.

²) A. J. Heins van der Ven, Philips techn. Rev. 5, 193, 1940.

³) Philips techn. Rev. 4, 267, 1939.

the two voltages, assumed to be purely sinusoidal are in a simple ratio — only in that case may we speak of a constant relative phase shift — a stationary Lissajous figure appears on the screen; in the simplest case, when the two voltages have the same frequency, it is an ellipse. From the form of the ellipse the phase angle can be deduced (*fig. 2a*). In practice use may be made of a stencil upon which a series of ellipses for different phase angles is drawn (fig. 2*b*); this stencil is laid on the fluorescent screen, and the required phase angle is found by interpolation. The accuracy of this method, however, is not very high. Moreover it covers a measuring region of only 180°, since the ellipses are repeated for larger angles. Instead of applying the two voltages directly to the deflection plates, the method can be made more sensitive by first deriving from one of them a voltage with a frequency eight times as great (see fig. 3). This is done, however, at the expense of the size of the measuring region. The Lissajous figure produced repeats the same series of shapes every $180/8 = 22^1/_2{}^\circ$, so that the method can only be used when it is a question of a small range of angles.

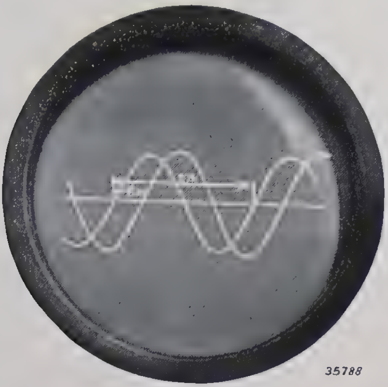

Fig. 1. With the help of an electron switch the variation with time of two quantities, for instance two voltages, can be shown simultaneously on the screen of a cathode ray oscillograph, so that the relative shift φ can be measured directly.

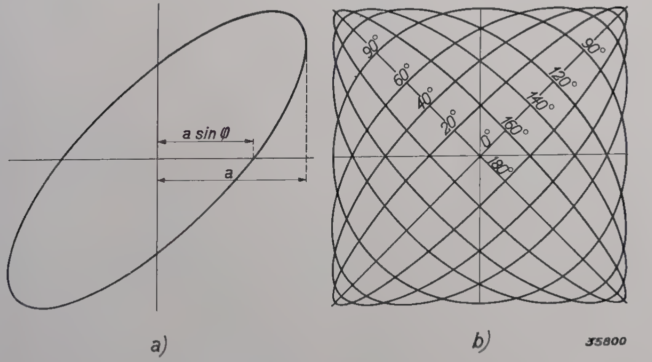

Fig. 2. *a*) From the shape of the ellipse which occurs on the screen with a phase shift φ of the two deflecting voltages of a cathode ray tube, the angle φ can be derived.
b) With the help of a stencil on which a series of ellipses are drawn the angle φ can be determined by interpolation.

An interesting possibility of measuring a phase angle is offered by a cathode ray tube in which the two directions of deflection of the electron beam are not always perpendicular, but can be adjusted to any desired angle. Such a tube can be realized by using for deflection two magnet coils placed against the neck of the tube (as is customary in television tubes [4])), one of which coils can be rotated through an angle α, which can be read off with respect to the other. If a current $i_0 \cos \omega t$ flows through the first coil, and through the second a current $i_0 \cos (\omega t + \varphi)$, in general an ellipse appears on the screen, whose character depends upon φ and the angle α, and which for $\alpha = \pi + \varphi$ passes over into a circle. The required angle φ is thus found as the (positive or negative) supplement of the angle α at which the movable magnet coil must be set in order to obtain a true circle on the fluorescent screen. This criterion permits quite a sharp setting, so that a measurement of φ is possible with an accuracy of a few degrees. The ranges of distinguishable angles is here also only 180° (because φ and $-\varphi$ lead to the same angle α).

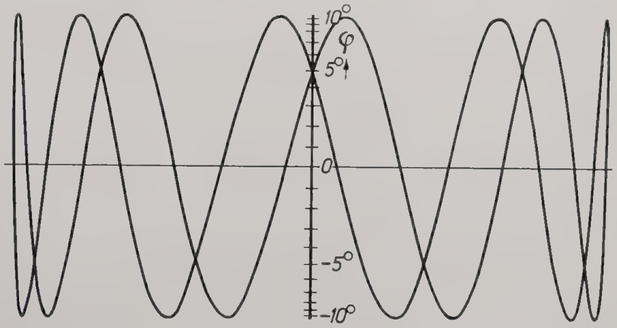

Fig. 3. Lissajous figure obtained by the deflecting voltage $\sin 8\,\omega t$ and $\sin (\omega t - \varphi)$; the angle φ can be read off on the scale. In this case $\varphi = 5°$.

Principles of the new method

Just as in the last method described, in the method worked out in this laboratory the phase difference is also directly visible as an angle, but in contrast to the above-described method the measuring range extends over all angles from 0 to 360°. The principle of the method is as follows (see the diagram of *fig. 4*).

To the two sets of deflection plates of an ordinary cathode ray tube two auxiliary voltages are applied which have the same frequency as the two given voltages whose phase difference is to be measured. Care is taken that the two auxiliary voltages have equal amplitudes and differ 90° in phase, so that the fluorescent spot describes a circle on the screen.

---

[4]) See Philips techn. Rev. **4**, 342, 1939, fig. 12.

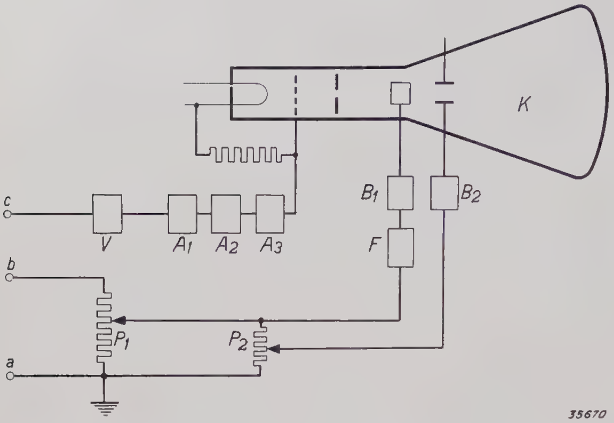

Fig. 4. Diagram of the new phase meter here described. An auxiliary voltage applied at *b* with the same frequency as the voltages to be compared is fed *via* two push-pull amplifiers B_1, B_2 to the two sets of deflection plates of a cathode ray tube *K*: By rotating the phase of one of the deflecting voltages 90° in the stage *F* and regulating the amplitudes with the potentiometers P_1 and P_2 the fluorescent spot is made to describe a circle. The voltages to be compared, applied successively to *c*, are fed *via* a regulatory amplifier *V* and three cut-off stages $A_{1,2,3}$, which are discussed in the text, to the regulatory electrode of the cathode ray tube, so that the beam current is modulated synchronously with the revolving light spot. The difference in position of the semi-circle on the fluorescent screen gives the phase difference of the voltages being compared.

One of the given voltages is now applied to the regulatory electrode (the grid) of the cathode ray tube. The beam current is hereby modulated in the same frequency as that of the deflecting voltages, *i.e.* the fluorescent spot is intense on one half of the circle traced and weak or invisible on the other half. The position of the greatest and of the smallest intensity, *i.e.* the position of the semi-circle (*fig.* 5) which is thus produced [5]), depends upon the phase of the modulating voltage with respect to the deflecting voltages. The same is repeated with the second given voltage. From the difference between the two positions of the semi-circle the required phase angle can be deduced.

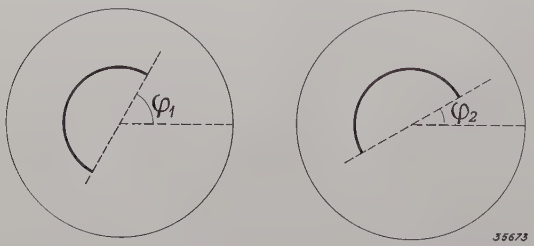

Fig. 5. Semi-circle on the fluorescent screen. If for one of the voltages this is at an angle φ_1 and for the other at the angle φ_2, the phase angle between the two voltages is $\varphi = \varphi_1 - \varphi_2$.

Practical application

Obtaining the circle

In order to obtain the circular motion of the fluorescent spot the same source of voltage is used as that from which the voltages whose phase is to be compared are taken. The voltage is on the one hand conducted to one set of deflection plates *via* a potentiometer and a push-pull amplifier [6]) and on the other hand it is rotated 90° in phase in a phase-rotating stage and conducted to the other set of deflection plates *via* a second push-pull amplifier. The connections of the phase-rotating stage are shown in principle in *fig. 6a*. As may be seen from the accompanying vector diagram (fig. 6*b*), a voltage is obtained between the terminals *3* and *4* whose phase with respect to the given input voltage (*1-2*) can be changed by variation of *R*.

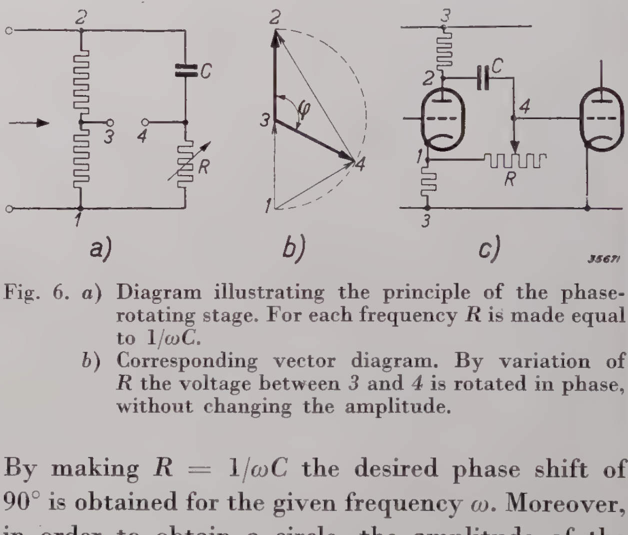

Fig. 6. *a*) Diagram illustrating the principle of the phase-rotating stage. For each frequency *R* is made equal to $1/\omega C$.
b) Corresponding vector diagram. By variation of *R* the voltage between *3* and *4* is rotated in phase, without changing the amplitude.

By making $R = 1/\omega C$ the desired phase shift of 90° is obtained for the given frequency ω. Moreover, in order to obtain a circle, the amplitude of the deflection voltage with rotated phase must always be equal to that with non-rotated phase. According to the vector diagram the connections of fig. 6 have the property that the amplitude of the rotated voltage (*3-4*) is not affected by the variation of the phase, which very much facilitates resetting to obtain a circle upon passing to another frequency.

The vector diagram — and thus the property mentioned — is only valid when no current is taken off between the terminals *3* and *4*. This is here approximately the case since the voltage *3-4* is fed to the grid of an amplifier valve. For practical reasons the connections are in reality made as represented in fig. 6*c*.

The modulated voltage

In order to be able to determine the position of the semi-circle on the fluorescent screen easily, it must break off sharply at the ends. This means that the voltage which modulates the intensity of the fluorescent spot must be very steep at the zero points. This is easily obtained with sufficient amplification of the (sinusoidal) voltage; at the same time, however, the cathode ray tube would be overloaded by the large amplitude of the regulatory voltage. This can be avoided simply by cutting off the peaks of the voltage: the originally sinusoidal voltage then has the shape of a "square sine" (*fig*. 7), and the curve representing the variation of the light intensity around the circumference of the circle on the fluorescent screen then has the same form.

---

[5]) A similar principle is applied in the apparatus of Balth. van der Pol and C. C. J. Addink (Philips techn. Rev. **4**, 205, 1939) for the rapid and accurate measurement of frequencies. Whether or not the semi-circle remains stationary is a very sharp criterion of the equality of the frequencies of the deflecting and modulating voltage.

[6]) The use of push-pull amplification is necessary in order to obtain a sharp image on the screen and in order to limit as far possible the distortion of the deflection voltages which would cause a deviation from true circular form.

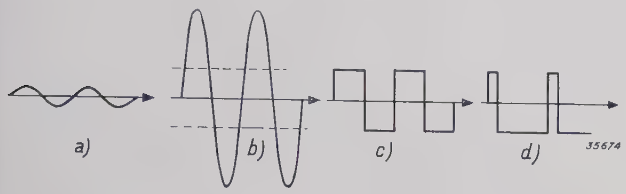

Fig. 7. The fronts of the sinusoidal voltage given (*a*) can be made sufficiently steep (*b*) by amplification, while at the same time the high peaks occurring are cut off at the level of the dotted line, so that a "square sine" (*c*) is obtained. If the levels given by the dotted lines are not symmetrical an asymmetrical "square sine" (*d*) occurs.

The connections given in *fig. 8a* (which serve at the same time for the desired amplification) serve to cut off the voltages. A sinusoidal A.C. voltage with large amplitude is applied to the terminals *1-3*. Whenever the voltage falls so far in the negative direction that the grid voltage v_g drops below the cut-off voltage v_m of the valve (fig. 8*b*) the anode current i_a remains zero until $v_g > v_m$ again. In this way the negative sine peaks are suppressed. Whenever the voltage in the positive direction increases so far that the grid potential becomes higher than the cathode potential, grid current begins to flow. The accompanying voltage decay over the resistance *r* makes the potential at *2* (the grid voltage) remain behind that at *1*, and with a sufficiently large value of *r*, the potential at *2* can never rise higher than the cathode potential, so that the anode current will already have the desired form.

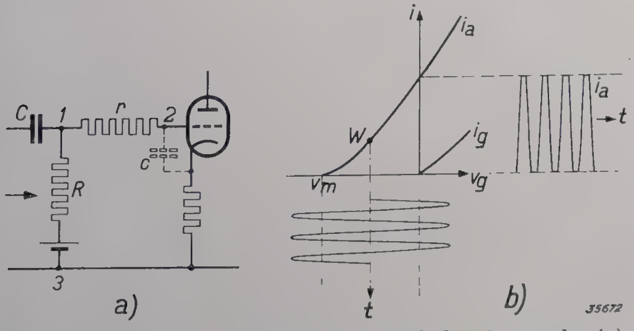

Fig. 8. Connections used for cutting off the sine peaks (*a*). If the voltage fed to *1-3* falls below the cut-off voltage v_m of the amplifier valve (*b*), the anode current i_a remains zero. If the voltage rises so that the potential at *2* reaches the cathode potential, grid current flows, and due to the voltage drop $i_g \cdot r$, the potential of *2* remains below that at *1*. With sufficiently high value of *r* the anode current will vary according to the desired "square sine" form.

In this connection the following must be noted. The zero level of the voltage applied, *i.e.* the operating point of the valve (*W* in fig. 8*b*) must lie halfway between the two constant levels (cut-off voltage and cathode potential) where the sine peaks are cut off. With an asymmetrical position of the zero level an asymmetrical "square sine" would occur (fig. 7*d*), and both ends of the semi-circle on the screen would be slightly lengthened or shortened. While it is true that the chord which joins the ends of the arc of the circle remains parallel to the original diameter so that the measurement is not unfavourably influenced with slight asymmetry, nevertheless with greater asymmetry the measurement would become very inaccurate. In the grid bias required for the correct position of the operating point the voltage decay $i_g \cdot R$ which is caused by the grid current i_g over the leakage resistance *R* must also be taken into account. The part of the grid bias which serves to compensate for this voltage drop is represented in fig. 8*a* by the battery shown in series with *R*.

With a given grid bias the correct position of the operating point is thus obtained only when the grid current has a certain mean value $\bar{i}_g$. The value of $\bar{i}_g$, however, depends closely upon the height of the sine peaks which must be cut off by the whole arrangement. If the connections are arranged for a given height of these peaks, *i.e.* for a given amplitude of the voltages whose phases are to be compared, and if a voltage with another amplitude is then fed to *1-3*, a discrepant i_g value occurs, the compensation of the voltage drop $\bar{i}_g R$ is not correct, and the operating point of the valve shifts until the positive voltage peaks projecting above cathode potential cause an $\bar{i}_g$ of the correct value. In order to avoid this shift, and the accompanying lengthening or shortening of the arc, the voltages to be compared must first be brought (at least approximately) to the constant amplitude for which the grid bias is calculated. We have done this by first feeding the voltages to an amplifier with automatic volume control which gives a practically constant output voltage with an input voltage between 6 mV and 3 V (maximum deviations 10 per cent).

Frequency region

It is stated above that with sufficiently high resistance r (fig. 8a) the potential at point 2 no longer increases to any extent as soon as grid current begins to flow. In practice, however, it is found impossible to give the resistance r such a high value as would be required for this. The cutting off of the sine peaks is therefore not complete, so that the anode current of the valve varies about as shown in *fig. 9b*. In order to make the remaining reduced sine peaks disappear and to obtain a true "square sine", two more stages like the one shown are connected behind the stage in fig. 8a.

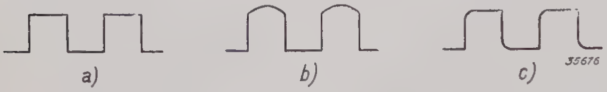

Fig. 9. If the resistance r in fig. 8a is not sufficiently high to cut off the sine peaks completely, instead of a "square sine" (a) we obtain a voltage variation which still has sine peaks, like curve (b). These are eliminated in the following cut-off stages. If an ideal "square sine" is applied to *1-3* of the last cut-off stage, then at point *2* due to the resistance r and the grid capacity c (fig. 8a), the potential cannot jump suddenly, and a rounding off of the curve is the result (curve c).

Let us now consider the last of these three stages. The voltage fed to this stage has almost the form of the "square sine"; the potential at point 1 therefore would at certain moments (corresponding to the beginning of the semi-circle visible on the screen) jump discontinuously from zero to a given value. Then, however, the potential of the grid (point 2) varies as a function of the time according to $1 - \exp(-t/rc)$, where c is the unavoidable grid capacity of the valve (indicated in fig. 8a by a dotted line). In fig. 9c this variation is shown. The round corner which makes the beginning of the semi-circle poorly defined can be described by a relaxation time proportional to rc. For satisfactory reading this relaxation time must amount to not more than a certain fraction, for instance $^1/_{100}$, of the whole period (circumference of the circle). From this it follows that the highest frequency at which satisfactory results can be obtained is inversely proportional to r. Naturally r cannot be made indefinitely small, since then the whole effect of the cut-off stage in question would become illusory. At the value of r chosen by us the rounding of the corners is not disturbing up to frequencies of about 100 000 c/s.

At the low-frequency end the frequency region in which the phase can be measured is limited due to a similar cause. If we again consider the last of the three cut-off stages, and again assume that in the one before the last an ideal "square sine" has been obtained, then due to the finite size of the coupling condenser C and the leakage resistance R in fig. 8a the variation of potential at point 1 will take on the form of *fig. 10b* (thin lines): the decrease of potential after each jump can be described by a relaxation time proportional to RC. As long as this time is large with respect to the period, the decrease is not disturbing, since the sine peaks are in any case cut off in the last stage according to the dotted line. At very low frequencies, however, the voltage represented in fig. 10c is obtained, which no longer gives a sharply ending semi-circle.

The lower frequency limit can be lowered by increasing R and C. In our case, where it was not particularly a question of low frequencies, the proportions were such that the lower frequency lay at about 100 c/s.

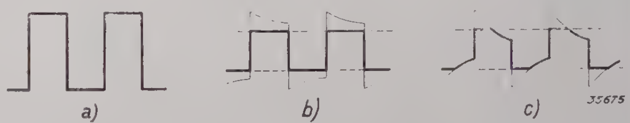

Fig. 10. If a "square sine" voltage (a) is supplied to the circuit of fig. 8a, the voltage at *1-3* varies according to (b) due to the limited size of R and C. As long as the downward sloping parts are cut off (b) this decay is not disturbing. At low frequencies, however, (b) gradually passes over to forms like (c) which cannot be used.

The apparatus as constructed

In *fig. 11* a photograph is given of the apparatus as constructed in this laboratory. The phase meter is mounted together with a tone generator which serves as voltage source for many measurements. Other details are given in the text under the figure. A celluloid plate which can be rotated with the help of a ring is placed directly over the screen. On this plate a set of parallel lines and a number of concentric circles are drawn (*fig. 12*). The latter serve for facilitating regulation of the circle which is obtained by adjusting the phase and amplitudes of the deflection voltages. When the circle has been obtained and given a suitable size [7]) (potentiometer P_1 in the diagram of fig. 4), the two voltages between which the phase angle is to be determined are fed in turn to the cut-off apparatus. By turning the ring with the celluloid plate so that the extremities of the semi-circle obtained fall upon one of the parallel straight lines the angle can be read off on a scale around the ring with an accuracy of $^1/_2$°.

By this method it is particularly easy to study the behaviour of filters. If the phase rotation is required which an input voltage of a given frequency undergoes in the different filter cells, the filter and the circle apparatus of the phase meter are supplied from the tone generator with the desired frequency, and the voltage behind each cell is successively tapped off and fed to the cut-off apparatus of the phase meter. In this way a series of semicircles is obtained in which the gradually increasing phase rotation is clearly demonstrated.

---

[7]) A suitable size is for instance a diameter of 8 cm. With the acceleration voltage of 2 000 V of the cathode ray here used — this high voltage is desirable in order to obtain a sufficiently high intensity of the image for measurement in a room which is not darkened — deflection voltages of about 200 V (peak value) are necessary.

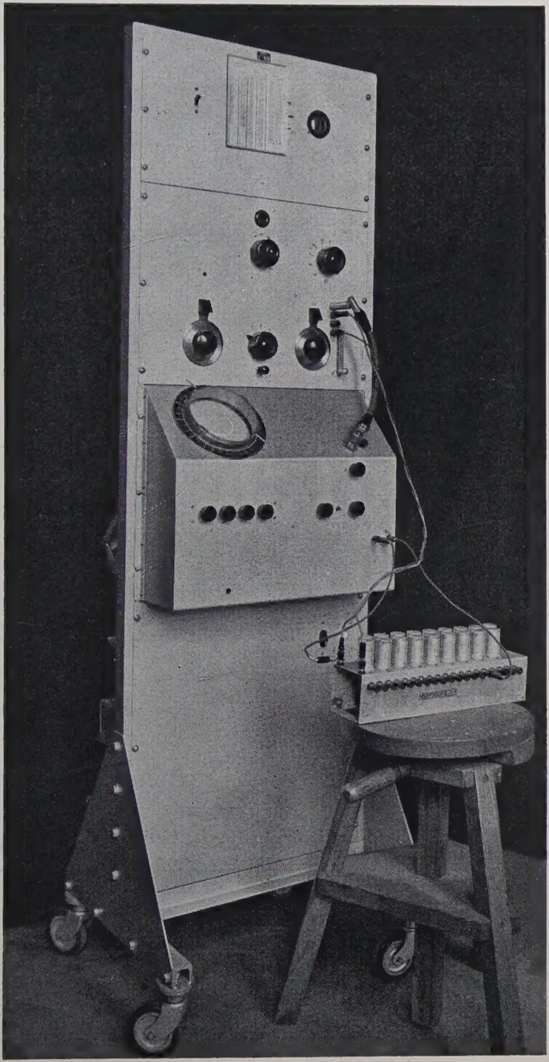

Fig. 11. The phase meter is mounted together with a tone generator (above) on one frame. To the left may be seen the screen of the cathode ray tube which is placed obliquely for easy reading. With the seven knobs below, the shape, size, position, sharpness and intensity of the circle on the screen are adjusted. To the right in front of the apparatus is a filter connected for measurement.

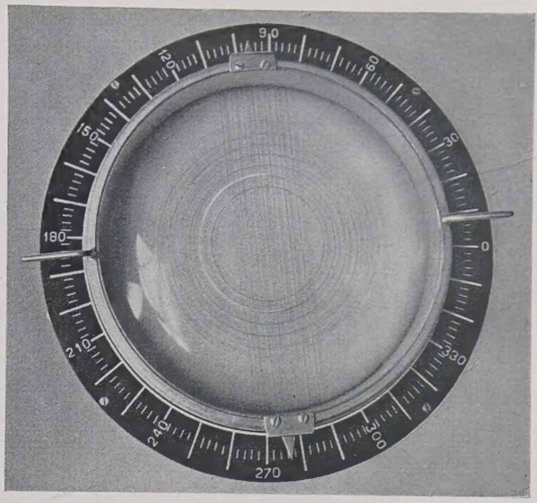

Fig. 12. Close-up of the fluorescent screen and of the celluloid plate over it which can be rotated by means of a ring. On the plate is a set of parallel lines and concentric circles. The ring bears a scale of angles.

Accuracy of measurement

It is clear that with a differential measurement any possible phase rotations in the regulatory amplifier and the cut-off connections of the phase meter have no effect on the results, when this rotation is the same for both the voltages to be compared. Since these voltages have the same frequency, they can only be distinguished by their amplitude (and their phase). In control measurements at 100 000 c/s. it has been found that in the whole range of amplitudes in which the measurement is possible, the phase rotation varies not more than 1° (see *fig. 13*).

Another possible source of error which we shall consider is a slight deviation of the image obtained on the screen from a true circle. The lighting up and dying out of the revolving light spot takes place at given moments t, and in our measurements we assume that ωt (aside from a multiple of 2π) is equal to the angle α at which the guiding ray of the light spot stands at the moment t. This is correct only as long as the spot traces a circle with constant velocity. Suppose that in adjusting the circle we had truely sinusoidal deflection voltages which were shifted exactly 90° in phase, but that in making the amplitudes equal we have made a slight error.

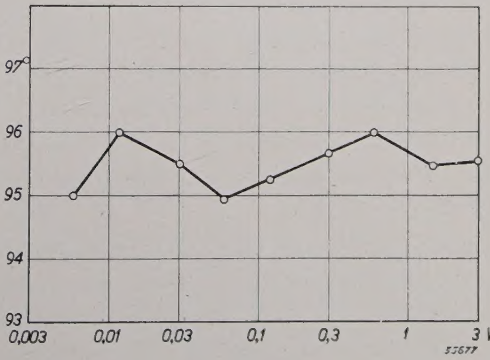

Fig. 13. For comparative phase measurements a phase rotation in the cut-off apparatus presents no difficulty when this rotation is independent of the amplitude. It is found that this requirement is satisfied for amplitudes between 6 mV and 3 V with an accuracy of 1°.

Let the horizontal deflection be

$$x = \cos \omega t$$

and the vertical: $y = (1 + \varepsilon) \sin \omega t$.

The angle α read off at moment t is given by:

$$\tan \alpha = y/x = (1 + \varepsilon) \tan \omega t$$

There is now a slight difference between α and ωt, which may be expressed approximately by:

$$\alpha - \omega t \approx \tan(\alpha - \omega t) = \frac{\tan \alpha - \tan \omega t}{1 + \tan\alpha \tan\omega t} =$$

$$= \frac{\varepsilon \tan \omega t}{1 + (1+\varepsilon)\tan^2 \omega t} \approx \frac{\varepsilon}{2} \sin 2\omega t.$$

The error in the phase angle read off is therefore $\varepsilon/2$ at the most. This can be understood more easily by considering the length r of the guiding ray of the light spot. This length is

$$r = \sqrt{x^2 + y^2} =$$

$$= \sqrt{1 + (2\varepsilon + \varepsilon^2) \cos^2 \omega t} \approx 1 + \varepsilon \cos^2 \omega t,$$

while with a perfect circle ($\varepsilon = 0$) r would equal one in the scale chosen. The maximum radial deviation from the circle of the figure obtained (ellipse) is thus ε, and it may be stated that the maximum error in the phase angle measured is one half the maximum deviation from circularity. If for instance the radius is 4 cm and the greatest radial deviation is 1 mm (this accuracy is easily attained), then $\varepsilon = 0.025$ and thus the possible error in the phase angle is 0.012, *i.e.* about $^3/_4$°. For other possible causes of deviations from the true circle, (harmonics, phase shift not exactly 90°) a similar estimation is found. Taking these considerations into account, the possible error in the comparative measurements described, in the frequency region 100 - 100 000 c/s and in the amplitude region 6 mV - 3 V, can be set at about 2°. The accuracy is the same for all angles between 0 and 360°.

An important property of the phase meter described, which we wish to point out in conclusion, is its slight sensitivity to interferences. Interfering voltages, if they are of a different frequency from the one examined, have no effect at all on the measurement, which is contrary to the case of almost all other methods. The hum voltage of 50 c/s. for instance, which often appears as interfering voltage, only makes the circumference line of the circle somewhat wider without changing its position. Interferences of the same frequency as the one being examined, for instance due to induction in the connections of the phase meter, must of course here also be avoided as in every method of phase measurement, since they affect the quantity to be measured itself.

TECHNICAL TEMPERATURE MEASUREMENT WITH THERMO-ELEMENTS

536.53

Nowadays in the preparation or working of almost every technically used alloy, the alloy is subjected to a carefully worked-out heat treatment, which has the purpose of influencing in a certain direction the mechanical, magnetic or other properties of the material. Such a heat treatment consists of heating the metal successively for definite times to definite, more or less accurately prescribed temperatures. The methods by which this is done will not be considered here, but we shall concentrate our attention on the problem of how these temperatures are controlled.

Since it is here a question of fairly high temperatures in general, for instance in the neighbourhood of 500 or 1000 °C, and since a rapid and simple measurement is required for such technical purposes, the thermo-element is the most suitable device. The thermo-voltage between the two contact metals whose junction has been brought to the temperature to be determined is measured by means of a galvanometer which need not be especially sensitive, since at temperatures of 500 °C for instance, with suitably chosen contact metals (for example chromel-alumel), thermo-voltages of 20 mV and more are obtained. The measuring instrument can be made of a registering type so that a continual control is possible of the whole heat treatment.

What is determined in such a thermo-electric measurement is in fact not a temperature, but a temperature difference. There must in any case always be a closed circuit, *i.e.* the two contact metals join not only at the welded junction but also at a second spot (indirectly perhaps, *via* one or more intermediate metals, see below). At this second "cold" junction there is an opposing EMF which depends upon the temperature of this point. The EMF measured is the difference between the two EMF's and therefore depends upon the difference in temperature of the two points of contact. If the indicating instrument is to be calibrated directly in temperature units, *the second contact must be kept at a definite constant temperature.*

How can this condition be satisfied? The air temperature is far from sufficiently constant, since in many cases the temperature must be determined to within a few degrees. In a laboratory it is customary to create a constant temperature artificially by means of melting ice; for routine measurements, however, this method would be too expensive. Instead of this use can be made of the fact that running water from the mains has a temperature which varies only slightly summer and winter. A still simpler method is obtained when one realizes the reason for the fact just mentioned: the pipe system of the water mains lies mainly underground and the water takes on the temperature of the ground through which it flows. This ground temperature is more or less constant (independent of the air temperature). An obvious solution is therefore to keep the cold contact of the thermo-elements at the desired constant temperature by putting it at some depth underground. This method is actually followed in the Philips factories.

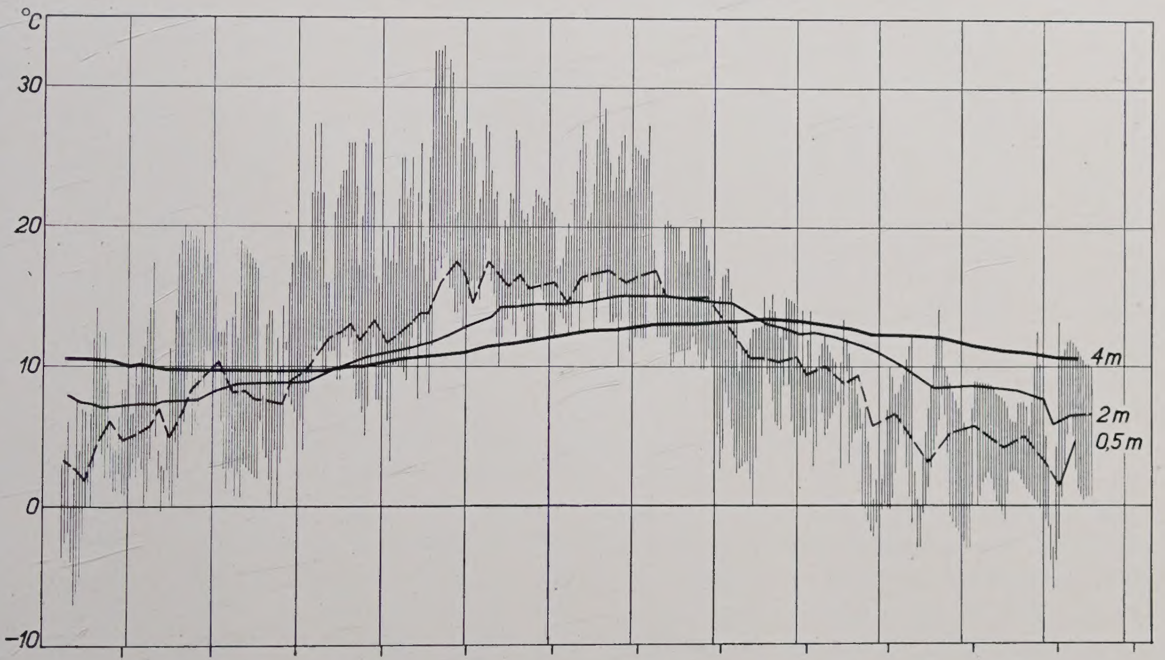

Fig. 1. Variation of the temperature of the ground at different depths during one year. For the sake of comparison the region between the maximum and minimum temperatures of the air, measured daily, is shaded. With increasing depth the amplitude of the yearly temperature fluctuation becomes smaller, while at the same time it exhibits a phase shift.

It is clear that the upper layer of soil will follow the temperature fluctuations of the air to a certain extent, or rather, to a certain depth. In order to discover at what depth the ground temperature no longer varies with time to any extent, the temperature of the soil at various depths on the grounds of this laboratory has been measured during a long time. For this purpose a series of narrow pipes of different lengths were driven into the ground. An ordinary mercury thermometer mounted in a copper block was lowered to the bottom of every pipe. Thanks to the large heat capacity of the copper block no appreciable error could occur during the daily pulling up and reading of the thermometers. In *fig. 1* the variation of temperature at 0.5 m, 2 m and 4 m depth measured in this way is given, while the region over which the air temperature varied is shaded. It is clear from the figure that the variations of the ground temperature become smaller with increasing depth, and moreover — an interesting and for the rest well-known phenomenon —, that the half-yearly temperature maxima and minima exhibit a certain shift, increasing with the depth, with respect to the temperature at the surface. This phase shift, which is a result of the delayed penetration of the sun's warmth due to the poor heat conduction of the soil, already amounts to about three months at a depth of 4 m. From experiments of other investigators it has been found that at a depth of about 8 m the phase shift is half a year, so that at that depth the highest temperature appears in December and the lowest in June.

We are mainly interested in the maximum temperature variations, which are plotted in *fig. 2* as a function of the depth. The broken line curve represents measurements by Tait in Edinburgh, which were carried out in quite a different type of soil. The conclusion to be drawn from the results of the measurements is that in general a depth of 4 m is enough, with if necessary a positive correction in the months March to May and a negative correction in the months September and October of 2° in the calibration of the thermo-elements. Under buildings the temperature variations are still smaller than in the measurements here described out of doors.

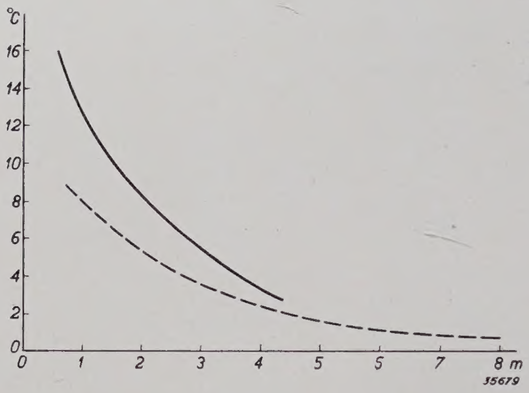

Fig. 2. The maximum temperature difference occurring during a year as a function of the depth. The full-line curve refers to measurements carried out in Eindhoven (sand ground), the broken-line curve gives the result of measurements by Tait (Edinburgh, porphyry rock).

In the practical application of the method a less pleasant consequence is the fact that the wires of the thermo-element would have to be very long in order to place the cold junction at the required depth in the ground. This is particularly unpleasant when the measurement of the EMF is not done by a compensation method as is in general the case with technical measurements. The alloys used for the thermo-element often have a fairly high specific resistance, so that with long lengths of wire the indication of the galvanometer becomes appreciably different from what it would be if only the resistance of the galvanometer were included in the circuit. The chromel-alumel elements, for instance, have a resistance of 0.23 ohm per metre length of the pair of wires with a thickness of wire of 2.3 mm.

Improvement can be achieved by the use of a socalled compensation connection. The latter consists of two metals which have a smaller electrical resistance than the contact metals of the thermo-element, and which are thermo-electrically equivalent to the latter, *i.e.* they give the same thermo-EMF without. however, needing to have the same great resistance to heat. In *fig. 3* is shown how the compensation connection is made. If we indicate the thermo-EMF between any two metals P and Q whose contact point has the temperature τ by E^{τ}_{PQ} (which then equals $-E^{\tau}_{QP}$), then the total thermo-EMF in the circuit of fig. 3 is:

$$E = E^{t}_{AB} + E^{x}_{BC} + E^{\Theta}_{CD} + E^{x}_{DA}, \quad . \quad . \quad (1)$$

where t is the temperature to be determined, Θ the constant temperature of the ground and x the unknown and varying air temperature of the points of connection of the compensation connection. Since, when $t = \Theta = x$, the total thermo-EMF is zero, then

$$E^{x}_{AB} + E^{x}_{BC} + E^{x}_{CD} + E^{x}_{DA} = 0.$$

Thus equation (1) becomes

$$E = E^{t}_{AB} - E^{\Theta}_{DC} + \left(E^{x}_{DC} - E^{x}_{AB}\right) \quad . \quad . \quad (2)$$

Therefore, except for a constant, the desired thermo-EMF E^{t}_{AB} is actually measured when the expression in parenthesis, which varies with x, disappears for all air temperatures x to be considered, *i.e.* when in this region the pair of metals DC is thermo-electrically equivalent to AB.

The chromel-alumel elements give, in the temperature region in which x may lie, *i.e.* between about 0 and 50 °C, a thermo-EMF of 0.0406 mV/°C. The combination constantan-copper can here be used as an easily conducting compensation connection. For a certain kind of constantan wire (the properties of constantan vary slightly according to the source), combined with normal electrolytic copper wire, we found a thermo-EMF of 0.0410 mV/°C, which corresponds very well with the value for chromel-alumel. The resistance of the compensation connection with a wire thickness of 2.5 mm amounted to about 0.1 ohm per m, and is therefore about $2^1/_2$ times as small as that of the chromel-alumel wires.

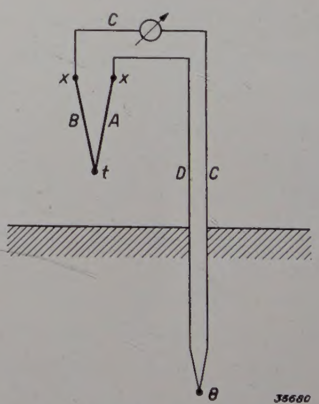

Fig. 3. In order not to be compelled to make the wires AB of the thermo-element very long, a compensation connection o two (thermo-electrically equivalent) metals C and D is joined to it, whose junction is given the constant ground temperature Θ. t is the temperature to be determined, x the air temperature of the connecting points of the compensation connection.